Entanglement in ultracold atomic gases

Author : **I. Morera** [1] ‡
Advisors : **Bruno Juliá-Díaz**[1,2,3], **and A. Polls**[1,2]

[1] Departament de Física Quàntica i Astrofísica, Facultat de Física, Universitat de Barcelona, Barcelona 08028, Spain
[2] Institut de Ciències del Cosmos, Universitat de Barcelona, ICCUB, Martí i Franquès 1, Barcelona 08028, Spain
[3] ICFO-Institut de Ciencies Fotoniques, The Barcelona Institute of Science and Technology, 08860 Castelldefels (Barcelona), Spain

Abstract. Ultracold atomic gases in optical lattices have provided a highly controllable environment in which many-body effects can be explored, going from weakly-interacting gases to strongly-correlated systems. Besides that, the recent development of quantum information theory has provided a new perspective for studying these systems, introducing entanglement notions which can fully characterize the phases at which the system can be found. In this work we want to provide an introduction to all these concepts using well-established theoretical techniques and comparing with numerical simulations carried out with a Density Matrix Renormalization Group (DMRG) algorithm.

First of all, we present a study of the single-component Bose-Hubbard model, using basic analytical theories, mean-field, perturbation theory, etc, accompanied with accurate DMRG results. We characterize the phase diagram with usual condensed-matter properties like the excitation spectrum but we also introduce entanglement properties like the von Neumann entropy. Furthermore, we perform a study of the two-component Bose-Hubbard where we present the entanglement spectrum (ES) of the system in the strong-coupling regime. Analytical results for the ES are obtained through perturbation theory and we also provide a direct comparison with DMRG results. At the critical point, where phase separation takes place, a drastic change on the ES structure is observed. We relate this new structure in the ES with the tower of states (TOS) expected in the energy spectrum of the Hamiltonian. We then study how these structures evolve with the system size and with the interactions between bosons as one approaches to the thermodynamic limit and the strong-coupling regime.

‡ imorerna7@alumnes.ub.edu

Contents

1. Introduction

Since the experimental discovery of Bose-Einstein condensation (BEC) [1, 2, 3] there has been a lot of effort to understand the physics of ultracold many-body quantum systems [4, 5]. Among the multiple scenarios where ultracold atoms have been studied one of the most intriguing ones is loading the atoms into an optical lattice [6]. This phenomena can be accurately described by Hubbard-type models, which are fundamental descriptions taking into account the interplay between kinetic energy and interactions. These type of models were originally introduced to study solid-state physics and strongly correlated systems [7, 8] (e.g. dynamics of electrons in solids), but they are just an approximation to the real dynamics. Instead, it turns out that the Bose-Hubbard model [9] is an accurate description of the physics in an ultracold atomic system trapped in an optical lattice. Moreover, the effective parameters of the system can be derived from microscopic principles and they can be controlled experimentally [6, 10]. Which allows for a study from the weakly interacting regime (where BECs have been conceived) to the strongly interacting regime. Not only that, the dimensionality of the system and its geometry can be modified and controlled [11, 12, 13], even the strength of the atomic interactions is tuned using the famous Feshbach resonance [14, 15, 16]. Then, ultracold atomic gases in optical lattices offer the possibility to study a wide variety of physical problems in an unprecedented controlled way [17, 10].

One of the most interesting phenomena in quantum many-body systems are quantum phase transitions (QPT) [18]. These are phase transitions which occur at zero temperature and are therefore driven solely by quantum fluctuations stemming from Heisenberg's uncertainty principle. The Bose-Hubbard model presents a QPT [19] due to the interplay between kinetic energy and interactions. Two different phases have been described: a superfluid phase (SF) and a Mott insulator (MI). Due to the high control on the parameters of the model, this phase transition has been studied over the last decades in an experimental and theoretical way and nowadays is one of the best established ones.

Since the development of quantum information theory there has been an effort to connect its tools to the physics of strongly correlated systems. Usually, QPT are characterized by a series of order parameters, properties of the excitation spectrum, etc. But quantum information theory has provided new magnitudes, mainly related with the entanglement of the system, which can characterize the different quantum phases of the system [20, 21, 22]. In the last decades a great deal of work has been performed in that direction, trying to introduce entanglement properties into condensed matter systems and see how universal they are. On the other hand, many-body physics has offered to quantum information theory the possibility for implementing the high controllability of those systems into the task of building a quantum computer [23].

2. Ultracold atoms in optical lattices

Optical lattices are created by interfering optical laser beams [24] and they act as external periodic potentials for ultracold atoms (fermions, bosons and mixtures). They have allowed to study many-body effects with an unprecedented level of precision and control, specifically there is a full control on the lattice dimensionality and geometry, the lattice depth controlling tunneling effects and the interactions between ultracold atoms [17].

2.1. Single-particle problem

The behavior of a single-particle in a periodic external potential is a standard problem in quantum mechanics. In this section, we concentrate on the one-dimensional case. However, the extrapolation to higher-dimensional systems is straightforward. The Schrödinger equation reads,

$$i\hbar\frac{\partial\phi(x,t)}{\partial t} = \left(-\frac{\hbar^2}{2m}\nabla^2 + V_{\text{opt}}(x)\right)\phi(x,t). \tag{1}$$

Since the optical potential has a periodicity $V_{\text{opt}}(x+a) = V_{\text{opt}}(x)$ our Hamiltonian will commute with the translation operator $\hat{T} = e^{-i\hat{p}a}$. Therefore, we can find simultaneous eigenfunctions of the two operators. According to Bloch's theorem [25]

$$\phi_q^{(n)} = e^{iqx}u_q^{(n)}(x), \tag{2}$$

where $u_q^{(n)}(x) = u_q^{(n)}(x+a)$ are Bloch wavefunctions satisfying the same periodicity than the optical lattice. Here q stands for the quasi-momentum of the particle, and is confined to the first Brillouin zone $-\pi/a < q < \pi/a$, and n denotes a quantum number characterizing the eigenstate (e.g. the band number). The Schrödinger Eq. (1) reduces to $H\phi_q^{(n)} = E_q^{(n)}\phi_q^{(n)}$ which yields to an equation for the Bloch wavefunctions

$$\left[\frac{(\hat{p}+\hbar q)^2}{2m} + V_{\text{opt}}(\vec{x})\right]u_q^{(n)}(x) = E_q^{(n)}u_q^{(n)}. \tag{3}$$

The typical optical lattice potential is $V_{\text{opt}}(x) = V_0\sin^2(kx)$ where $k = \pi/a$, it has a periodicity a where $2a$ is the wavelength of the laser light. V_0 is the depth of the optical lattice and it is an experimental parameter that can be tuned. A typical characteristic frequency of the system is the trapping frequency defined as $w_T = \sqrt{4V_0E_R}/\hbar$ where $E_R = \hbar^2k^2/(2m)$ stands for the recoil energy [6]. In Fig. 1 we represent the band structure for different optical depths V_0. The case $V_0 = 0$ is a trivial one which represents the free particle with a quadratic spectrum. As long as V_0 is increased the band gap increases and the band width decreases. The typical band gap between the two lowest bands is characterized by the energy $\hbar w_T$.

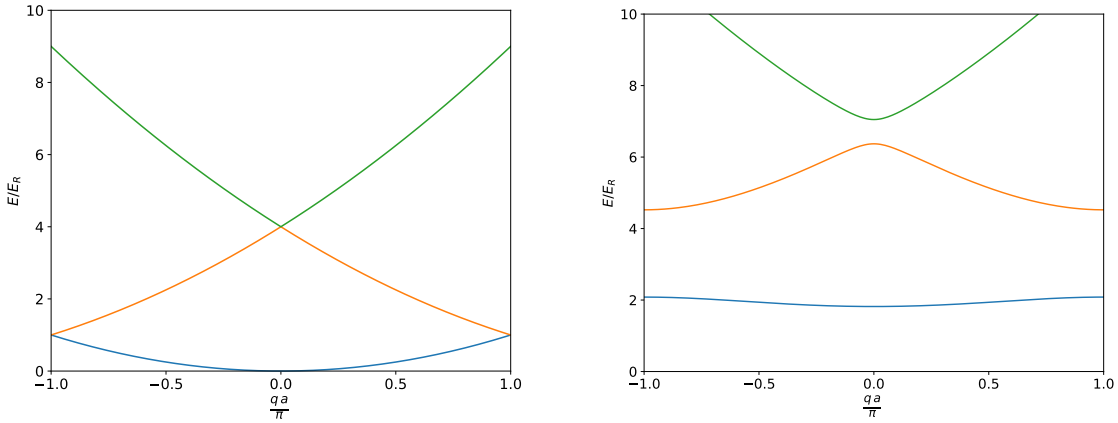

Figure 1. Band structure in a typical optical lattice acting as an external periodic potential $V_{\text{opt}}(x) = V_0 \sin^2(kx)$. On the left the untrapped case $V_0 = 0$ and on the right a trapped one with $V_0 = 5E_R$.

2.2. Microscopic derivation of the Bose-Hubbard model

Once the problem of the single-particle in an optical lattice is solved we can focus on the many-body problem. In the language of second quantization the many-body Hamiltonian describing a gas of N interacting bosons is given by [26]

$$\hat{H} = \int d\mathbf{r}\hat{\Phi}^\dagger(\mathbf{r}) \left[-\frac{\hbar^2}{2m}\nabla^2 + V_{\text{opt}}(\mathbf{r})\right] \hat{\Phi}(\mathbf{r}) + \frac{1}{2}\int d\mathbf{r}d\mathbf{r}'\hat{\Phi}^\dagger(\mathbf{r})\hat{\Phi}^\dagger(\mathbf{r}')V(\mathbf{r}-\mathbf{r}')\hat{\Phi}(\mathbf{r})\hat{\Phi}(\mathbf{r}'), \tag{4}$$

where the optical lattice $V_{\text{opt}}(\mathbf{r}) = \sum_{i=1}^{3} V_{i,0}\sin^2(kx_i)$ is a 3-dimensional generalization of the one described in the previous section. We have introduced $\hat{\Phi}(\mathbf{r})$ and $\hat{\Phi}^\dagger(\mathbf{r})$, the bosonic annihilation and creation field operators, respectively. In a general way, they are defined as

$$\begin{aligned} \hat{\Phi}(\mathbf{r}) &= \sum_n \phi_n(\mathbf{r})\hat{b}_n, \\ \hat{\Phi}^\dagger(\mathbf{r}) &= \sum_n \phi_n^*(\mathbf{r})\hat{b}_n^\dagger. \end{aligned} \tag{5}$$

The coefficients $\phi_n(\mathbf{r})$ and $\phi_n^*(\mathbf{r})$ are single-particle wavefunctions corresponding to the n eigenstate and $\hat{b}_n$, $\hat{b}_n^\dagger$ are the bosonic annihilation and creation operators. If $\{\phi_n(\mathbf{r})\}$ forms a complete basis, the field operators obey the commutation relations $\left[\hat{\Phi}^\dagger(\mathbf{r}), \hat{\Phi}(\mathbf{r}')\right] = \delta(\mathbf{r}-\mathbf{r}')$.

The interaction $V(\mathbf{r}-\mathbf{r}')$ plays a key role in the many-body problem. In the context of ultracold atoms, many degrees of freedom are frozen and the scattering of two particles can be reduced to only s-wave channels. In this situation, the exact shape of the interparticle two-body potential is not needed and it can be replaced by a short-

ranged pseudopotential [27, 28]

$$V(\mathbf{r}-\mathbf{r}') = \frac{4\pi\hbar^2 a_s}{m}\delta(\mathbf{r}-\mathbf{r}'), \tag{6}$$

being m the atomic mass and a_s the s-wave scattering length. The scattering length a_s characterizes the strength of the interactions: attractive (repulsive) for negative (positive) values and it can be tuned in present experiments by using Feshbach resonances [14, 15, 16]. Usually one defines the coupling constant as $g = \frac{4\pi\hbar^2 a_s}{m}$ and the many-body Hamiltonian is reduced to

$$\hat{H} = \int d\mathbf{r}\hat{\Phi}^\dagger(\mathbf{r})\left[-\frac{\hbar^2}{2m}\nabla^2 + V_{\text{opt}}(\mathbf{r})\right]\hat{\Phi}(\mathbf{r}) + \frac{g}{2}\int d\mathbf{r}\hat{\Phi}^\dagger(\mathbf{r})\hat{\Phi}^\dagger(\mathbf{r})\hat{\Phi}(\mathbf{r})\hat{\Phi}(\mathbf{r}). \tag{7}$$

In the dilute regime ($na_s \ll 1$ being n the gas density) the above problem can be approximately solved using the Bogoliubov approximation [29]. This consists in writing the field operators as a sum of a mean value and a fluctuation $\hat{\Phi}(\mathbf{r}) = \Phi(\mathbf{r}) + \delta\hat{\Phi}(\mathbf{r})$. Using the Heisenberg picture and neglecting quantum and thermal fluctuations an evolution equation for the mean value can be obtained, the so-called Gross-Pitaevskii equation [30, 31] which is a good approach for zero temperature and assumes that all bosons condensate.

Since we are interested in the many-body problem where the external potential is given by a periodic optical lattice it is convenient to expand the field operators in Bloch functions

$$\hat{\Phi}(\mathbf{r}) = \sum_{n,q}\phi_q^{(n)}(\mathbf{r})\hat{b}_q^{(n)}. \tag{8}$$

Another complete orthogonal basis is provided by the Wannier functions w_n [32]. Using these functions, the Bloch ones can be rewritten as

$$\phi_q^{(n)}(\mathbf{r}) = \sum_i e^{i\mathbf{q}\mathbf{r_i}}w_n(\mathbf{r}-\mathbf{r_i}), \tag{9}$$

where $\mathbf{r}_i = i\mathbf{a}$ is the lattice position. Wannier functions are not uniquely defined since Bloch functions are defined up to a global phase, which introduces large changes on Wannier functions. This freedom is often used to obtain highly localized functions at the point $\mathbf{r_i}$ which rapidly decay away from it. Taking into account this consideration, the field operator is rewritten

$$\hat{\Phi}(\mathbf{r}) = \sum_{n,i} w_n(\mathbf{r}-\mathbf{r}_i)\hat{b}_i^{(n)}, \tag{10}$$

and it can be interpreted as annihilating a particle at position $\mathbf{r}$. On the other side, $\hat{b}_i^{(n)}$ is the annihilation operator of a particle in the proper Wannier state $w_i^{(n)}(x)$ at site i and band n. Working in the ultracold regime we consider that the energies of our system are not enough to provoke excitations over different bands which are separated by the typical trapping frequency $w_T = \sqrt{4E_R V_0}/\hbar$ previously introduced (see Fig. 1),

then we are mainly left with the lowest band, $n = 0$. Introducing the expansion (10) on the Hamiltonian (7) we obtain

$$\begin{aligned} H = &\sum_{i,j} \hat{b}_i^\dagger \hat{b}_j \int d\mathbf{r}\, w^*(\mathbf{r}-\mathbf{r}_i) \left[-\frac{\hbar^2}{2m}\nabla^2 + V_{\text{opt}}(\mathbf{r}) \right] w(\mathbf{r}-\mathbf{r}_j) \\ &+ \frac{g}{2} \sum_{i,j,i',j'} \hat{b}_i^\dagger \hat{b}_{i'}^\dagger \hat{b}_j \hat{b}_{j'} \int d\mathbf{r}\, w^*(\mathbf{r}-\mathbf{r}_i) w^*(\mathbf{r}-\mathbf{r}_{i'}) w(\mathbf{r}-\mathbf{r}_j) w(\mathbf{r}-\mathbf{r}_{j'}), \end{aligned} \tag{11}$$

where we have dropped the band index since we only consider the lowest one ($n = 0$). As the Wannier functions are localized at a particular site i and rapidly fall away from the site (approximately exponential decay) we will neglect contributions such that $|i-j| > 2$ for the first integral, which is equivalent to consider tunneling only between nearest neighbors. We can also neglect offsite interactions for the second integral and only consider on-site interactions ($i = i' = j = j'$). With these assumptions we obtain the famous Bose-Hubbard Hamiltonian

$$H = -\sum_{<i,j>} t_{ij} \left(\hat{b}_i^\dagger \hat{b}_j + h.c. \right) + \frac{U}{2} \sum_i \hat{n}_i(\hat{n}_i - 1) + \sum_i \epsilon_i \hat{n}_i, \tag{12}$$

where we identify the following parameters:

$$\begin{aligned} t_{ij} &= \int d\mathbf{r} w^*(\mathbf{r}-\mathbf{r}_i) \left[-\frac{\hbar^2}{2m}\nabla^2 + V_{\text{opt}}(\mathbf{r}) \right] w(\mathbf{r}-\mathbf{r}_j), \\ U_i &= g \int d\mathbf{r} |w(\mathbf{r}-\mathbf{r}_i)|^4, \\ \epsilon_i &= \int d\mathbf{r} w^*(\mathbf{r}-\mathbf{r}_i) \left[-\frac{\hbar^2}{2m}\nabla^2 + V_{\text{opt}}(\mathbf{r}) \right] w(\mathbf{r}-\mathbf{r}_i), \end{aligned} \tag{13}$$

which describe a tunneling matrix, an on-site interaction and an inhomogeneous term, respectively. If the external optical potential is isotropic (as it will be in our case) the subindexes can be omitted and ϵ_i can be dropped out. Finally, let us emphasize that this Hamiltonian will describe the physics of ultracold atoms in periodic optical lattices if the condition $U, t, k_B T \ll \hbar w_T$ is fulfilled, which is the case in current experiments [6]. The most important point of this derivation is that the parameters of the Hamiltonian (12) are directly controlled by the depth of the optical lattice V_0 and the recoil energy E_R, then we have a high experimental control on the physics of the system.

3. Physics of the Bose-Hubbard model

The Bose-Hubbard model is considered one of the minimal models which includes many-body effects. It is a convenient point to start developing the quantum many-body theory which includes concepts like entanglement, quantum phase transitions, etc. As we have said, there has been an enormous technological progress and presently we have a very large experimental control on the parameters characterizing the model. The control is such that one can use these systems as quantum simulators, both from the experimental and theoretical point of view, of the physics in other fields: spin systems, etc [33].

It is important to realize that the Bose-Hubbard Hamiltonian contains a competition between kinetic energy introduced by the tunneling term t and the on-site interactions U. The kinetic energy tends to delocalize particles over the lattice. If this term dominates, the ground state of the system is in a superfluid (SF) phase. This one is characterized by large fluctuations in the number of particles per site, a divergent correlation length (critical phase) and a gapless spectrum. In the limit $t/U \to \infty$ we can write an exact superfluid wavefunction for the ground state with M lattice sites and N bosons

$$|\Psi_{SF}\rangle = \left(\frac{1}{\sqrt{N}}\sum_{i=1}^{M}\hat{b}_i^\dagger\right)^N |0\rangle. \tag{14}$$

In the limit $N, M \to \infty$ at fixed N/M the wavefunction tends to

$$|\Psi_{SF}\rangle = \prod_{i=1}^{M}\left[e^{\hat{b}_i^\dagger}|0\rangle_i\right], \tag{15}$$

which is nothing else than a coherent state for each site (an eigenfunction of $\hat{b}_i$) and a superposition of different particle number on each site following a Poisson distribution. In the opposite limit $t/U \to 0$ we found a total localization of particles in each site. The ground state has a well defined number of particles per site and it can be written as a Fock state with commensurate filling $n = N/M$

$$|\Psi_{MI}\rangle = \prod_{i=1}^{M}(\hat{b}_i^\dagger)^n|0\rangle. \tag{16}$$

This phase is called the Mott Insulator (MI) and is characterized by a finite correlation length and a gapped spectrum.

As we have seen the Bose-Hubbard model (12) presents a ground state with very different properties as a function of the ratio t/U. One expects that these two regimes will not be continuously connected and a QPT will appear at a finite value of t/U. In the following sections we will present a study of different properties deeper inside each phase and we will characterize the QPT between them.

3.1. Superfluid phase

In this section we show how to deal with the Bose-Hubbard model Eq. (12) near the non-interacting limit $t/U \to \infty$. In order to do that, we perform a Bogoliubov approximation [34, 35]. In this non-interacting limit all bosons condensate into the zero momentum state and the number of bosons occupying this state (N_0) is equal to the total number of bosons N. Using this information we rewrite the Bose-Hubbard Hamiltonian introducing new operators $\hat{b}_{\mathbf{k}}$

$$\hat{b}_i = \frac{1}{\sqrt{M}} \sum_{\mathbf{k}} \hat{b}_{\mathbf{k}} e^{i\mathbf{k}\mathbf{r}_i}, \tag{17}$$

where $\mathbf{r}_i$ represents the position of the site i and $\mathbf{k}$ is the momentum discretized over the first Brillouin zone. Using the fact that $\sum_i e^{-i(\mathbf{k}-\mathbf{k}')\mathbf{r}_i} = M\delta_{\mathbf{k},\mathbf{k}'}$ we obtain the total number of bosons as $\hat{N} = \sum_i \hat{b}_i^\dagger \hat{b}_i$. In the Bogoliubov approach one expands the bosonic operators using a mean-field approach $\hat{b}_{\mathbf{k}} = \sqrt{N_0}\delta_{\mathbf{k},0} + \delta\hat{b}_{\mathbf{k}}$ and substituting in the Hamiltonian Eq. (12) (in the grand canonical ensemble) one obtains, up to quadratic fluctuation terms

$$\begin{aligned} H = N_0 \left(-zt - \mu + \frac{U}{2}\right) + \sqrt{N_0}\left(-zt - \mu + Un_0\right)\left(\hat{b}_0 + \hat{b}_0^\dagger\right) \\ + \sum_{\mathbf{k}} \left(\epsilon_{\mathbf{k}} - \mu\right) \hat{b}_{\mathbf{k}}^\dagger \hat{b}_{\mathbf{k}} + \frac{Un_0}{2} \sum_{\mathbf{k}} \left(4\hat{b}_{\mathbf{k}}^\dagger \hat{b}_{\mathbf{k}} + \hat{b}_{\mathbf{k}}\hat{b}_{-\mathbf{k}} + \hat{b}_{-\mathbf{k}}^\dagger \hat{b}_{\mathbf{k}}^\dagger\right), \end{aligned} \tag{18}$$

where $n_0 = N_0/M$ is the condensate density fraction, z is the number of nearest-neighbors. The lattice dispersion reads as $\epsilon_{\mathbf{k}} = -2t\sum_i^d \cos(k_i a)$ where we are considering a general d-dimensional lattice.

Linear terms in bosonic operators can be removed setting the chemical potential to $\mu = Un_0 - zt$. This expression tells us that the necessary energy to add a particle into the system is given by the on-site interactions between the added boson and the n_0 bosons at each site, minus the energy due to the possible hopping to one of the z first-neighbors. Then the Hamiltonian of Eq. (18) is rewritten as

$$\begin{aligned} H = -\frac{Un_0 N_0}{2} + \sum_{\mathbf{k}} \left(\epsilon_{\mathbf{k}} + zt - Un_0\right) \hat{b}_{\mathbf{k}}^\dagger \hat{b}_{\mathbf{k}} \\ + \frac{1}{2} Un_0 \sum_{\mathbf{k}} \left(4\hat{b}_{\mathbf{k}}^\dagger \hat{b}_{\mathbf{k}} + \hat{b}_{\mathbf{k}}\hat{b}_{-\mathbf{k}} + \hat{b}_{-\mathbf{k}}^\dagger \hat{b}_{\mathbf{k}}^\dagger\right). \end{aligned} \tag{19}$$

This quadratic Hamiltonian can be solved using the so-called Bogoliubov-de Gennes transformation

$$\begin{pmatrix} \hat{c}_{\mathbf{k}} \\ c_{-\mathbf{k}}^\dagger \end{pmatrix} = \begin{pmatrix} u_{\mathbf{k}} & v_{\mathbf{k}} \\ v_{\mathbf{k}}^* & u_{\mathbf{k}}^* \end{pmatrix} \begin{pmatrix} \hat{b}_{\mathbf{k}} \\ a_{-\mathbf{k}}^\dagger \end{pmatrix}, \tag{20}$$

where the new operators $\hat{c}_{\mathbf{k}}, \hat{c}_{\mathbf{k}}^\dagger$ represent quasiparticle fields which follow the commutation rules $\left[\hat{c}_{\mathbf{k}}, \hat{c}_{\mathbf{k}'}^\dagger\right] = \delta_{\mathbf{k},\mathbf{k}'}$ and the coefficients satisfy the normalization

condition $|u_{\mathbf{k}}|^2 - |v_{\mathbf{k}}|^2 = 1$. Using these new operators the Hamiltonian of Eq. (19) is written as:

$$H = -\frac{Un_0N_0}{2} + \frac{1}{2}\sum_{\mathbf{k}} \left(\hbar w_{\mathbf{k}} - \epsilon_{\mathbf{k}} - zt - Un_0\right) + \sum_{\mathbf{k}} \hbar w_{\mathbf{k}} \hat{c}^\dagger_{\mathbf{k}} \hat{c}_{\mathbf{k}}, \tag{21}$$

where we have required that off-diagonal terms vanish, leading to the conditions

$$\begin{aligned} &\left(u^2_{\mathbf{k}} + v^2_{\mathbf{k}}\right) Un_0 - 2\left(\epsilon_{\mathbf{k}} + Un_0 + zt\right) u_{\mathbf{k}} v_{\mathbf{k}} = 0, \\ &\left(|u_{\mathbf{k}}|^2 + |v_{\mathbf{k}}|^2\right)\left(\epsilon_{\mathbf{k}} + Un_0 + zt\right) - Un_0\left(u^*_{\mathbf{k}} v_{\mathbf{k}} + u_{\mathbf{k}} v^*_{\mathbf{k}}\right) = \hbar w_{\mathbf{k}}. \end{aligned}$$

Using the normalization condition for $u_{\mathbf{k}}$ and $v_{\mathbf{k}}$ we find the solution

$$\begin{aligned} \hbar w_{\mathbf{k}} &= \sqrt{\left(\epsilon_{\mathbf{k}} + zt\right)^2 + 2Un_0\left(\epsilon_{\mathbf{k}} + zt\right)}, \\ |v_{\mathbf{k}}|^2 &= |u_{\mathbf{k}}|^2 - 1 = \frac{1}{2}\left(\frac{\epsilon_{\mathbf{k}} + zt + Un_0}{\hbar w_{\mathbf{k}}} - 1\right). \end{aligned} \tag{22}$$

In the long-wavelength limit $|\mathbf{k}|a \ll 1$ the quasiparticles behave as phonons with a dispersion

$$\hbar w_{\mathbf{k}} \approx |\mathbf{k}| a \sqrt{t} \sqrt{t|\mathbf{k}|^2 a^2 + 2Un_0}, \tag{23}$$

showing the gapless nature of the spectrum in the SF phase, note that this approach cannot characterize the MI phase which is gapped.

Within the Bogoliubov approach the original system is described in terms of quasiparticles with an annihilation operator $\hat{c}_{\mathbf{k}}$ and a characteristic excitation spectrum $\hbar w_{\mathbf{k}}$. At zero temperature the vacuum of the system fulfills $\hat{c}_{\mathbf{k}}|\text{vac}\rangle = 0$. At non-zero temperature different excited states are occupied through thermal activation, satisfying the well-known Bose-Einstein statistics

$$\langle \hat{c}^\dagger_{\mathbf{k}} \hat{c}_{\mathbf{k}} \rangle = \frac{1}{e^{\beta \hbar w_{\mathbf{k}}} - 1}. \tag{24}$$

One can compute the average filling at non-zero temperature as

$$n = \frac{\langle N \rangle}{M} = \frac{1}{M} \sum_{\mathbf{k}} \langle \hat{b}^\dagger_{\mathbf{k}} \hat{b}_{\mathbf{k}} \rangle. \tag{25}$$

Using the Bogoliubov-de Gennes transformation Eq. (20) and the thermal occupation of the quasi-particles Eq. (24) we obtain:

$$n = n_0 + \frac{1}{M} \sum_{\mathbf{k} \neq 0} \left[\left(|u_{\mathbf{k}}|^2 + |v_{\mathbf{k}}|^2\right) \frac{1}{e^{\beta \hbar w_{\mathbf{k}}} - 1} + |v_{\mathbf{k}}|^2 \right], \tag{26}$$

where we have separated the filling contribution in two parts: n_0 which represents the condensate contribution to the total filling and the contribution from higher non-condensate states. Using Eq. (22) we obtain

$$n = n_0 + \frac{1}{M} \sum_{\mathbf{k} \neq 0} \left(\frac{\epsilon_{\mathbf{k}} + zt + Un_0}{\hbar w_{\mathbf{k}}} \frac{1}{e^{\beta \hbar w_{\mathbf{k}}} - 1} + \frac{\epsilon_{\mathbf{k}} + zt + Un_0}{2\hbar w_{\mathbf{k}}} - \frac{1}{2} \right). \tag{27}$$

At zero temperature $\beta \to \infty$ the term with the thermal occupation goes to zero and taking the continuum limit analytical results can be obtained depending on the dimensionality of the system. The strategy is to see at fixed integer filling number n the amount of condensation n_0 that is present in the system. It is expected that at finite t/U there will be a critical point where n_0 goes to zero and this will mark the SF-MI phase transition. Here we do not provide the full derivation and just sum up the main results depending on the dimension of the system. In $d = 2, 3$ the system does not show any critical point at finite t/U at which the condensation goes to zero, only the limit $t/U \to 0$ shows a vanishing condensation $n_0 = 0$ since there is no hopping parameter. That leads to the conclusion that the Bogoliubov approach is unable to predict a QPT from SF to MI (it only works when $n \sim n_0$) and a more sophisticated formulation has to be performed as we will see in following sections. An special case is the one-dimensional one, where the integration over momenta diverges, which indicates that there are no true Bose-Einstein condensates in one-dimensional systems. This is formalized in the Mermin-Wagner-Hohenberg theorem [36, 37, 38], where it is shown that there are no Bose-Einstein condensates at any temperature in one-dimensional systems and only at zero temperature in two-dimensional systems. The assumption that there is Bose-Einstein condensation in these forbidden situations leads to the conclusion that it must have an infinite density, which is inconsistent. Note that the non-existence of Bose-Einstein condensation does not forbid the existence of a SF phase. In fact, superfluidity does not require the existence of a Bose-Einstein condensate with a totally coherent phase, it only requires a quasi-condensation [39].

3.2. Mott Insulator phase

Before introducing a theory which can capture the transition from MI to SF we will inspect some properties of the pure MI phase. In the limit $t/U = 0$ the Hamiltonian Eq. (12) can be decomposed as a sum of single sites. Therefore we will study only the single site problem

$$h = \frac{U}{2}\hat{n}(\hat{n} - 1) - \mu\hat{n}. \tag{28}$$

This Hamiltonian is directly diagonal in the basis of eigenstates of the particle number operator $\hat{n}|n\rangle = n|n\rangle$, then $h|n\rangle = \epsilon_n|n\rangle$ where

$$\epsilon_n = \frac{U}{2}n(n - 1) - \mu n. \tag{29}$$

The ground state $|n_0\rangle$ of the system can be found minimizing ϵ_n with respect to the particle number n. This leads to the condition on the number of particles

$$\begin{cases} n_0 = 0 & \text{if} \quad \mu \leq 0 \\ n_0 - 1 \leq \left[\frac{\mu}{U}\right] \leq n_0 & \text{if} \quad \mu \geq 0, \end{cases} \tag{30}$$

where [.] stands for the minimum integer part greater than the argument. This shows that the number of bosons per site is a step function of the chemical potential, denoting the incompressible nature of the MI phase.

3.3. Mean-field approach

In previous sections we have studied specific properties of the Bose-Hubbard model (12) in two limiting cases $t/U \to \infty, 0$. However, this can not explain how the transition between these two phases takes place. Therefore, we have to develop a method to solve the Hamiltonian for any value of t/U. The most straightforward technique is the so-called mean-field approach. The basic idea is to replace the many-body interactions with an effective mean-field which reduces the problem to a single-particle. This can be achieved by expanding operators in terms of fluctuations around their expectations values (similar to the Bogoliubov approach). In the Bose-Hubbard model (12) we can expand bosonic operators

$$\begin{aligned} \hat{b}_i^\dagger &= \psi^* + \delta\hat{b}_i^\dagger, \\ \hat{b}_i &= \psi + \delta\hat{b}_i, \end{aligned} \tag{31}$$

where ψ^* and ψ represent the expectation value of the bosonic operators $\hat{b}_i^\dagger$ and $\hat{b}_i$, respectively and $\delta\hat{b}_i^\dagger$, $\delta\hat{b}_i$ represent quantum fluctuations over these expectation values. Note that we have omitted a lattice position index for the mean values since we are assuming an homogeneous effective field for the whole lattice. Now we can rewrite the tunneling term of the Hamiltonian (12)

$$\hat{b}_i^\dagger\hat{b}_j = \left(\psi^* + \delta\hat{b}_i^\dagger\right)\left(\psi + \delta\hat{b}_j\right) \approx |\psi|^2 + \psi^*\left(\hat{b}_j - \psi\right) + \psi\left(\hat{b}_i^\dagger - \psi^*\right) = \psi\hat{b}_i^\dagger + \psi^*\hat{b}_j - |\psi|^2, \tag{32}$$

where we have omitted second-order fluctuation terms. In this way, we can rewrite our Hamiltonian in the grand-canonical ensemble as a mean-field one

$$H_{MF} = \sum_i \left(\frac{U}{2}\hat{n}_i\left(\hat{n}_i - 1\right) - \mu\hat{n}_i - 2tz\left(\psi^*\hat{b}_i + \psi\hat{b}_i^\dagger\right) - 2tz|\psi|^2\right) = \sum_i h_i, \tag{33}$$

where z is the number of nearest-neighbours and μ is the chemical potential. Note that we have decoupled the tunneling term between nearest-neighbours, then the problem has been reduced to a single-site one and we only have to solve the single-particle Hamiltonian h_i, this technique is often called site-decoupling mean-field.

Notice that the original Hamiltonian (12) was invariant under a global U(1) phase transformation $\hat{b}_i \to \hat{b}_i e^{i\phi}$ which leads to the particle number conservation. But the mean-field Hamiltonian (33) breaks this symmetry as long as $\psi \neq 0$. This is a reminiscence that the Bose-Hubbard has two different phases: one respecting the U(1) symmetry with $|\psi| = 0$ (MI) and another one breaking U(1) with $|\psi| \neq 0$. Therefore $|\psi|$ can be seen as an order parameter characterizing the phase transition.

Following Landau theory [40] one can write the ground state energy in a general form in powers of the order parameter $|\psi|$

$$E = a_0 + a_2|\psi|^2 + a_4|\psi|^4 + \mathcal{O}(|\psi|^6). \tag{34}$$

The MI phase will be stable as long as $a_2 \geq 0$, since the minimization of the energy leads to $\psi = 0$ and there is a unique ground state. For $a_2 < 0$ the previous mentioned

ground state becomes unstable and the ground state becomes infinitely degenerated with a non-vanishing $\psi \neq 0$. The symmetry of the system is spontaneously broken selecting a particular phase value and we will be in the SF phase. Then, the critical line can be obtained through the condition $a_2 = 0$.

In order to explicitly obtain the coefficients in Eq. (34) we perform a perturbation theory writing $h = h_0 + h_1$ where $h_1 \propto t \ll U$

$$\begin{aligned} h_0 &= \frac{U}{2}\hat{n}\left(\hat{n}-1\right) - \mu\hat{n}, \\ h_1 &= -2tz\left(\psi^*\hat{b} + \psi\hat{b}^\dagger\right) + 2tz|\psi|^2. \end{aligned} \tag{35}$$

The unperturbed ground state energy is easily obtained $E^{(0)}(n) = \frac{U}{2}n\left(n-1\right) - \mu n$ which is just the energy of the pure MI, Eq. (29). Now, the first-order in perturbation theory is zero because the expectation value of h_1 over the MI ground state vanishes. The second order is given by

$$E^{(2)} = 2tz|\psi|^2 + \sum_{n\neq n_0} \frac{|\langle n_0|h_1|n\rangle|^2}{E^{(0)}(n_0) - E^{(0)}(n)}, \tag{36}$$

where $|n_0\rangle$ ($|n\rangle$) represents the ground state (an excited state) with well-defined number of particles n_0 ($|n\rangle$). The matrix elements are given by

$$\begin{aligned} \langle n_0|h_1|n_0+1\rangle &= -2tz\psi^*\sqrt{n_0+1}, \\ \langle n_0|h_1|n_0-1\rangle &= -2tz\psi\sqrt{n_0}, \end{aligned} \tag{37}$$

and we obtain the second order correction to the ground state energy

$$E^{(2)} = 2tz|\psi|^2 + (2tz)^2|\psi|^2\left(\frac{n_0+1}{\mu - Un_0} - \frac{n_0}{\mu - U\left(n_0-1\right)}\right). \tag{38}$$

Once obtained the explicit form of Eq. (34), the condition at which $a_2 = 0$ reads

$$\frac{1}{2zt} = \frac{n_0}{\mu - U\left(n_0-1\right)} - \frac{n_0+1}{\mu - Un_0}, \tag{39}$$

and two branches can be obtained representing particle and hole excitations

$$\mu_\pm = -zt \pm \sqrt{(zt)^2 - 2zt\left(n_0+1/2\right) + U^2/4}. \tag{40}$$

In Fig 2 we represent the phase diagram obtained through the critical lines Eq. (40). It exhibits different Mott lobes with fixed number density $n_0 = 1, 2, 3, ...$ and the tip is characterized by the condition $\mu_+ = \mu_-$ which leads to

$$\frac{zt_c}{U} = 2n_0 + 1 - 2\sqrt{n_0(n_0+1)}. \tag{41}$$

This gives an approximate value for the tip of the first lobe $zt_c/U \approx 0.17$. In general, the tip of the lobes is an special type of point, let's see why. Employing the Landau

theory, Eq. (34), at fourth order, the minimization of the energy for the SF phase leads to

$$E = a_0 - \frac{a_2^2}{2a_4}. \tag{42}$$

The boson density $\bar{n} = -\partial E/\partial\mu$ is given by

$$\bar{n}_{SF} = -\frac{\partial a_0}{\partial\mu} + \frac{a_2}{2a_4}\frac{\partial a_2}{\partial\mu} - \frac{a_2^2}{2a_4^2}\frac{\partial a_4}{\partial\mu}. \tag{43}$$

For the MI phase ($\psi = 0$) following a similar procedure we obtain $\bar{n}_{MI} = -\partial a_0/\partial\mu$ then, at the SF phase the boson density can be expressed as

$$\bar{n}_{SF} = \bar{n}_{MI} + \frac{a_2}{2a_4}\frac{\partial a_2}{\partial\mu} - \frac{a_2^2}{2a_4^2}\frac{\partial a_4}{\partial\mu}, \tag{44}$$

which leads to the result that the phase transition from MI to SF leads to a change on the boson density. This is true except when

$$\frac{\partial a_2}{\partial\mu} - \frac{a_2}{a_4}\frac{\partial a_4}{\partial\mu} = 0, \tag{45}$$

which is fulfilled at the tip of the lobes $\partial a_2/\partial\mu = 0$. Then this is the point where the transition from MI to SF is accompanied by a constant boson density. From these expressions is easy to verify that the MI corresponds to an incompressible phase since $\partial\hat{n}_{MI}/\partial\mu = 0$.

In this section we have seen that the site-decoupling mean-field approach can give insights about the phase diagram of the Bose-Hubbard model, shown in Fig. 2. As long as the dimension of our system is large, the mean-field approach will be better, being an exact approach for an infinite dimensional system. Then for one-dimensional or quasi one-dimensional systems where quantum fluctuations are very suppressed in transverse directions we do not expect that the mean-field approach will be a reliable one.

3.4. A DMRG study

As we have anticipated the physics of one-dimensional quantum systems can be really different from the multidimensional ones. A very efficient method to deal with the peculiarities of the one-dimensional system is the so-called Density Matrix Renormalization Group (DMRG). The basic idea of the DMRG (and any other numerical renormalization technique [41]) is that in order to describe the physics of some many-body system we do not need to know the full Hilbert space, instead we can remove some degrees of freedom from our system and truncate the full Hilbert space. Indeed, starting from a well-known microscopic Hamiltonian the size of the system is increased and new degrees of freedom are added up while others are integrated out, thus modifying the real Hamiltonian to an effective and simpler one which can capture the physics of the system.

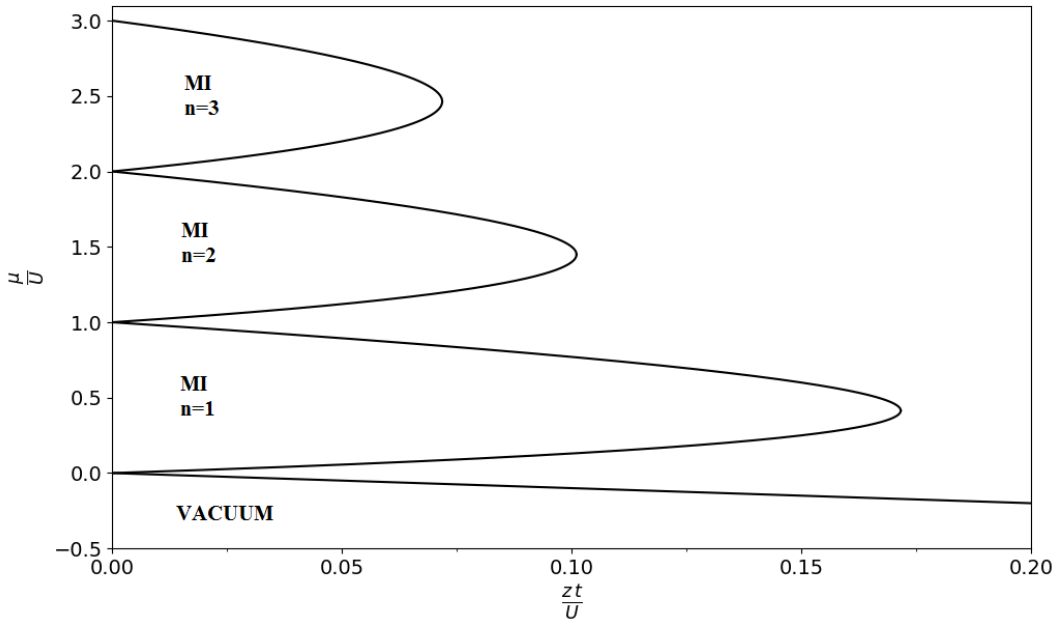

Figure 2. Mean-field phase diagram of the Bose-Hubbard model Eq. (12) in the plane $\mu/U - zt/U$.

From this basic idea many different methods have been proposed, but in this work we will focus on the traditional approach introduced by White [42]. The main idea is to perform a truncation of the full Hilbert space retaining a finite number of states which maximally contribute to the reduced density matrix. A fully detailed review presenting the method can be found in [43], also see [44] for a more pedagogical introduction.

Despite the fact that DMRG was created as a numerical renormalization group nowadays it has been reinterpreted as a variational method in the subspace of matrix product states (MPS) [45]. Indeed, the ground state and elementary excitations of a system can be expressed in the thermodynamic limit as a proper matrix product state ansatz which can be updated through a variational method. Quantum information theory has provided insights about the efficiency of DMRG, connecting it directly with the entanglement of the system [46, 22, 47]. From this, it has been realized that one-dimensional systems, critical or not, can be efficiently simulated with DMRG being this one the most powerful methods to deal with these systems. From this discovery, the introduction of tensor networks has opened a range of possibilities for extensions of the DMRG, allowing one to simulate the real time evolution of systems [48] and simulate multi-dimensional systems, despite this is still an open problem since they are subjected to an area law [49, 50].

From the DMRG perspective the Bose-Hubbard model presented in Eq. (12) can be efficiently simulated in the one-dimensional context and exact results can be obtained and compared with our analytical solutions. Our study will be performed using the

characteristic $U(1)$ symmetry that presents this system, leading to the conservation of number of bosons. This will not allow us to obtain the full phase diagram in the plane $\mu/U - t/U$, since we are working in the canonical ensemble, but the exact tip point of MI lobes where the transition from MI to SF is produced at constant boson density, as we have seen in previous sections. We will work at commensurate density $\rho = N/L = 1$ then we are examining the phase transition from MI to SF in the first Mott lobe.

As we have seen this transition corresponds to go from an incompressible to a compressible phase, thus, it can be identified by measuring the energy cost of adding a particle or a hole

$$\begin{aligned} \mu_c^+ &= E_0(N = L + 1) - E_0(N = L), \\ \mu_c^- &= E_0(N = L) - E_0(N = L - 1), \end{aligned} \tag{46}$$

where $E_0(N = L)$ is the ground state energy with fixed number of bosons $N = L$. This defines a particle-hole excitation gap, namely $\Delta_c = \mu_c^+ - \mu_c^-$, which characterizes the incompressible MI phase by $\Delta_c \neq 0$ and the compressible SF phase by $\Delta_c = 0$. At constant density in d dimensions the MI-SF transition is on the (d+1) XY universality class [9]. In a one-dimensional system this leads to a Berezinskii-Kosterlitz-Thouless (BKT) type transition for which the energy gap closes asymptotically according to [9]

$$\Delta \sim e^{-\frac{C}{|\sqrt{t_c - t}|}}, \tag{47}$$

where C is some non-universal constant and t_c is the critical point at which the transition is produced.

The DMRG requires a truncation on the number of states which are kept (defined as m) based on the eigenvalues of the reduced density matrix [42]. The error introduced by the DMRG method is directly related to the weights of the discarded eigenvalues in the truncation process. In our situation we have observed that this error depends on the phase in which the system is found. This is directly related to the entanglement of the system. The SF phase is a gapless critical one characterized by an infinite correlation length, for finite systems this correlation length is of the order of the system size and one needs a huge number of m eigenvalues to describe the system which increases with the system size. On the other hand the MI has a finite correlation length and there is no dependence on the system size, being tractable with DMRG with a few number of states kept. In our simulations, we have taken $m = 100$ states and all the obtained results are giving with an error lower than 10^{-8}. Another truncation which has to be performed in a bosonic system is to put a cuttof on the maximum number of bosons per site. This cuttof has to be taken such that the finite number of bosons per site does not affect the results. A convergence study has been performed, obtaining that allowing for a maximum of five bosons per site is enough to obtain a convergence of the same order than the one introduced by the truncation error in DMRG.

Using DMRG (with open boundary conditions) we obtain the particle and hole excitations Eq. (46) for finite systems. In Fig. 3 we show the scaling for the energy

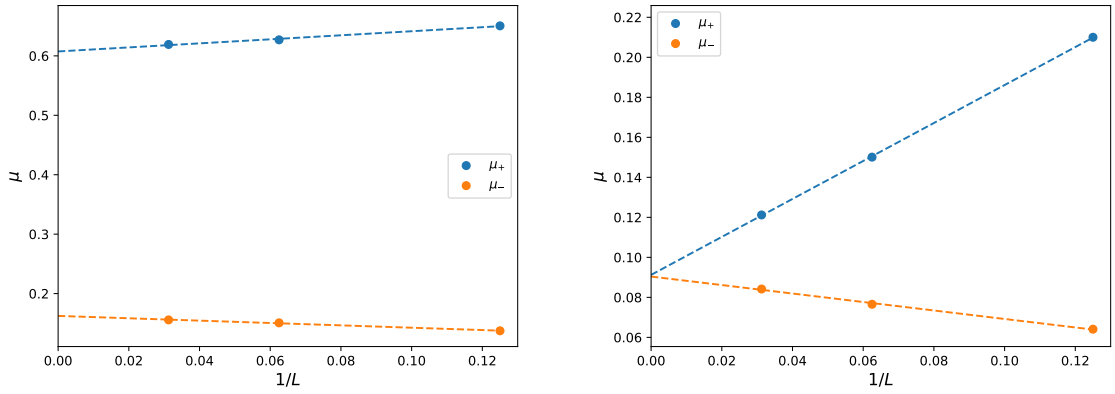

Figure 3. Chemical potential as a function of the system's size. On the left (right) we represent a case in the Mott insulator phase $t/U = 0.1$ (near the critical point $t/U = 0.3$). The upper set of points corresponds to the energy required to add a particle to the system μ_c^+ and the lower one to the energy of adding a hole μ_c^+. Dashed lines are linear fits to the numerical results.

of the particle and hole excitations for two different values of the ratio t/U. We have extracted a leading scaling as $1/L$ for the two type of excitations. Deep inside the MI phase the scaling is very weak and the properties of the system do not depend so much on the system size, just opposed to the SF phase. From this scaling we can obtain the energy gap Eq. (46) in the thermodynamic limit as is depicted in Fig. 4. We can obtain the critical point at which the MI-SF is produced characterizing the closure of the gap Eq. (46) which leads to the value $t_c = 0.30 \pm 0.01$. This value is compatible with the ones obtained through Monte Carlo studies [51], exact diagonalization [52] and other DMRG studies [53, 54, 55, 56]. We have to emphasize that these values are very different from the one predicted by the mean-field calculation in previous sections. As we have pointed out we did not expect that the mean-field approach would capture the physics of the one-dimensional system.

Among different measures that have been defined in order to measure the amount of entanglement in a system one of the most useful ones is the von Neumann entropy. Given a system which can be decomposed into two subsystems, namely A and B, the total Hilbert space can be defined as the product $\mathcal{H} = \mathcal{H}_A \otimes \mathcal{H}_B$ and any state can also be decomposed as $|\psi\rangle = \sum_i \alpha_i |\phi_i^A\rangle \otimes |\phi_i^B\rangle$ which is usually called a Schmidt decomposition. The coefficients α_i are positive defined and are called Schmidt values and if $|\psi\rangle$ is properly normalized they satisfy that $\sum_i \alpha_i^2 = 1$. The states $\{|\phi_i^A\rangle\}$ ($\{|\phi_i^B\rangle\}$) are orthonormal sets of $\mathcal{H}_A$ ($\mathcal{H}_B$). One can also define the reduced density matrix of the subsystem A as $\rho_A = \mathrm{Tr}_B \rho$, where Tr_B means to tracing out the subsystem B and ρ is the density matrix of the full state $\rho = |\psi\rangle\langle\psi|$. Using the Schmidt decomposition one can write

$$\rho_A = \sum_{\phi_i^B} \langle \phi_i^B | \psi \rangle \langle \psi | \phi_i^B \rangle = \sum_i |\alpha_i|^2 |\phi_i^A\rangle \langle \phi_i^A|. \tag{48}$$

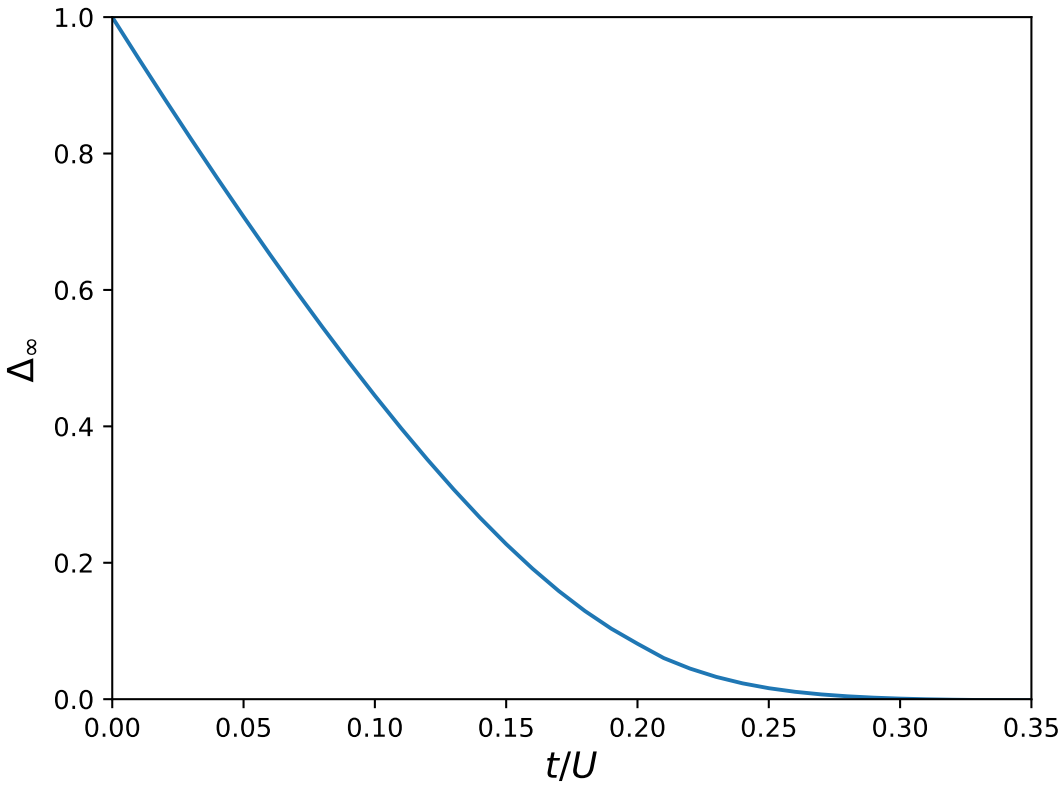

Figure 4. Particle-hole excitation gap Δ_c as a function of the ratio t/U. The data is presented in the thermodynamic limit extrapolated using linear fits as the ones presented in Fig. 3.

The von Neumann entropy associated with the Schmidt values is defined as a Shannon entropy

$$S_{VN} = -\sum_i \alpha_i^2 \log \alpha_i^2, \tag{49}$$

and it is a direct measure of the entanglement between the two subsystems A and B. If the total state can be written as a product state $|\psi\rangle = |\phi^A\rangle \otimes |\phi^B\rangle$ then the von Neumann entropy is null $S_{VN} = 0$, since there is only one Schmidt value with $\alpha = 1$ and there is no entanglement in the system. On the other hand fully entangled systems have m equal Schmidt values $\alpha = 1/\sqrt{m}$, being $m = \min(\dim(\mathcal{H}_A, \mathcal{H}_B))$, and the von Neumann entropy has a value $S_{VN} = \log m$.

The von Neumann entropy Eq. (49) has been used in many analysis of different physical situations. Therefore, it turns out to be a useful magnitude to characterize a system. In a critical system characterized by a correlation length $\xi \to \infty$, the low-lying spectrum (long-distance physics) can be explained from a 1+1 Quantum Field Theory (QFT) perspective, specifically from a massless one, a Conformal Field Theory (CFT) [57]. In this situation the von Neumann entropy for a system with total size L

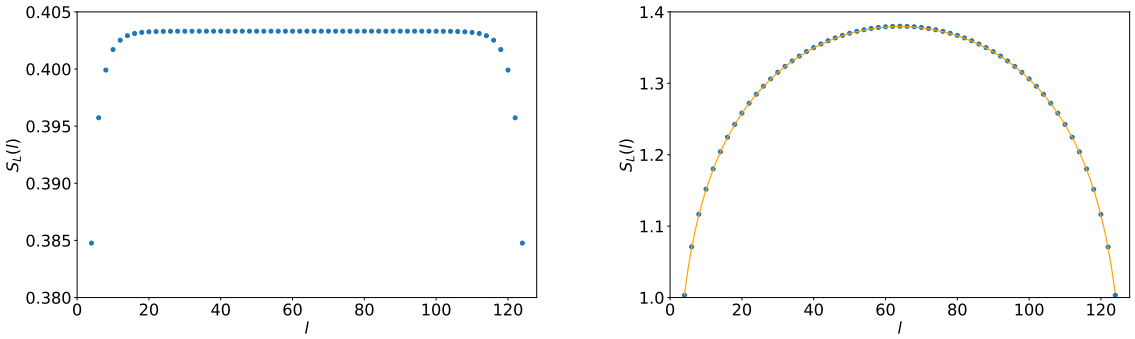

Figure 5. von Neumann entropy $S_L(l)$ at fixed total size $L = 128$ as a function of the subsystem size l. On the left we show case deep inside the Mott insulator regime $t/U = 0.15$ and on the right in the superfluid one $t/U = 0.4$. The continuous orange line on the right panel represents the CFT analytical result, Eq. (50), with central charge $c = 0.97$.

with open boundaries, divided in some subsystem A with size l reads as [58, 59]

$$S_L(l) = \frac{c}{6} \log \left(\frac{L}{\pi} \sin \frac{\pi l}{L} \right) + \log g + c_1^{'}, \tag{50}$$

where c is the central charge characterizing the underlying CFT, $\log g$ is a boundary entropy contribution [60] and $c_1^{'}$ is some non-universal constant. On the other hand, for massive 1+1 QFT (with an energy gap) the von Neumann entropy will saturate due to the finite correlation length $S_L(l) \sim \log \xi$ [58]. Additional contributions to Eq. (50) which go beyond the CFT universality have been found. These are Friedel-like oscillations [61, 62] due to the open boundary condition, which decay away from the boundary.

As we have seen the SF phase is characterized by being a critical one, in fact, the low energy physics in the one-dimensional context can be described by the Luttinger liquid theory [63] which is a CFT with central charge $c = 1$. On the other hand, the MI phase has a finite correlation length and we expect a saturation of the von Neumann entropy at the point $l \gg \xi$. In Fig. 5 we show the von Neumann entropy $S_L(l)$ for a system with $L = 128$ for two different values of the ratio t/U, one corresponding to a SF case and other to the MI one. The von Neumann entropy is obtained at fixed total size L and varying the size l of the subsystem A. In the SF case our results are very well described by Eq. (50), oscillation terms are expected at the boundaries, but we can safely ignore them and obtain a value for the central charge $c = 0.97$ which is in very good agreement with the analytical result. On the other hand, for the MI phase the von Neumann entropy rapidly saturates for increasing values of the subsystem length l, this remarks the gapped nature of the MI phase associated with a finite correlation length.

Knowing the behavior of the entanglement in the two phases, now we can try to determine the critical point using just the von Neumann entropy. In order to do that

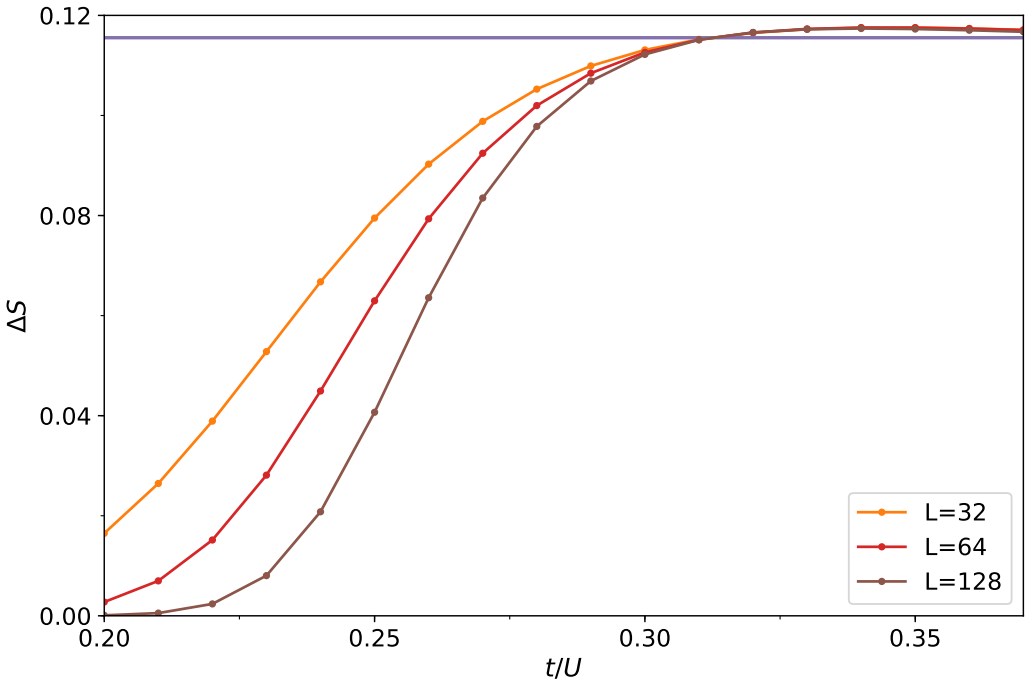

Figure 6. Dashed lines represent the magnitude $\Delta S = S_L(L/2) - S_L(L/4)$ as a function of the ratio t/U for different system's sizes L. The continuous line gives the CFT prediction $\Delta S = c\log(2)/6$ which is expected to be followed at the superfluid regime with central charge $c = 1$. Deviations from the CFT prediction are expected at small systems due to the open boundary conditions.

we investigate the scaling of the entropy at a subsystem size $l = L/2$ and varying the total size $L \to 2L$ [64]

$$\Delta S = S_L(L/2) - S_L(L/4). \tag{51}$$

We expect that the SF phase follows the CFT behavior, $\Delta S = (c/6)\log 2$ following Eq. (50). For the MI phase we have seen that the entropy saturates due to the finite correlation length, then we expect that $\Delta S = 0$ for $L \gg \xi$. In Fig. 6 we represent ΔS as a function of the ratio t/U for different system sizes. For increasing values of t/U different curves corresponding to different system sizes converge to the CFT prediction, small deviations from that are due to finite size effects. On the other hand, for lower values of t/U the curves tend to zero as the system size L is increased, revealing the gapped nature of the MI. One should expect a step function-like behavior in the thermodynamic limit, where $\Delta S = 0$ as long as we are in the MI regime and $\Delta S = (c/6)\log 2$ in the SF one. We can see that different curves intersect the CFT result in the range (close to $t/U = 0.31$) where we have predicted the MI-SF transition using the energy gap $t_c = 0.30 \pm 0.01$, revealing an agreement between the two procedures: the one analyzing the energy gap and the one resulting from entanglement properties.

4. Two-component Bose-Hubbard model

A simple multicomponent bosonic system can be realized using two different hyperfine states of the same element [65]. These systems have been loaded into optical lattices [66, 67, 68] and it has been shown that are accurately described by a Bose-Hubbard Hamiltonian, which not only takes into account the interplay between kinetic energy and interactions for each species but it also includes a local coupling between the two species. In these systems we have extra degrees of freedom with respect to the single-component one, so a richer phase diagram is expected [69, 70, 71]. Specifically, among the MI and SF phase in the two-component system a phase separated one has been found [72, 73] and the effect of an extra linear coupling term between the two components has been studied [74, 75]. These phenomena have been experimentally observed in [76] using two hyperfine states of Rb. Understanding the entanglement in these multicomponent systems is still a challenge. Recent studies have considered the entanglement between two components for a largely imbalanced case [77, 78].

The extended Bose-Hubbard model has two different types of bosons, in a 1D optical lattice can be written in a second quantized form as,

$$\begin{aligned} H = &- \sum_{<i,j>} \left(t_A \hat{b}_{iA}^\dagger \hat{b}_{jA} + t_B \hat{b}_{iB}^\dagger \hat{b}_{jB} + \text{h.c.} \right) + \\ &+ \frac{1}{2} \sum_i \left(U_A \hat{n}_{iA} \left(\hat{n}_{iA} - 1 \right) + U_B \hat{n}_{iB} \left(\hat{n}_{iB} - 1 \right) \right) + \\ &+ U_{AB} \sum_i \hat{n}_{iA} \hat{n}_{iB}, \end{aligned} \tag{52}$$

where $\hat{b}_{i\sigma}$ ($\hat{b}_{i\sigma}^\dagger$) are the annihilation (creation) bosonic operators at site i for species $\sigma = A, B$, respectively, and $\hat{n}_{i\sigma}$ are their respective number operators. The first line represents the tight-binding Hamiltonian with hopping parameters t_A and t_B for each species and $< i, j >$ represents a sum over nearest-neighbors. The second line represents intracomponent on-site interactions with strength U_A and U_B. The last line represents the local coupling between the two components. For the rest of the work we consider $t_A = t_B = t > 0$ and $U_A = U_B = U > 0$ and we will set the energy scale to $t = 1$.

In the following section we perform a study in the strong-coupling regime $U \gg t$ varying the intercomponent interaction U_{AB} in the range $U_{AB} \in [0, U]$. We characterize the entanglement between two subblocks of the total system and we relate the entanglement properties with the physics of the system.

4.1. Entanglement spectrum in the two-component Bose-Hubbard model

As we have seen, entanglement properties like the von Neumann entropy allow to characterize different phases of the system. But this is a single number that comes from an entire spectrum provided by the reduced density-matrix, and one should expect to have more information encoded in this spectrum. This was first proposed by Li and

Haldane in [79] where they defined the entanglement spectrum (ES) $\xi_i = -\log \lambda_i$, which is the spectrum coming from the so-called entanglement Hamiltonian $\mathcal{H}_E \equiv -\log \rho_A$, where ρ_A is the reduced density matrix associated to the subsystem A Eq. (48). Despite the fact that the ES only contains information of the degrees of freedom of the subsystem A [64, 80], there is a conjecture speculating that there is a correspondence between the ES and the energy spectrum of the real Hamiltonian [81, 82]. Recent investigations have provided further insights into this direction showing the boundary-like character of the ES for gapped systems [83] and the bulk-nature at critical points and the correspondence with a CFT spectrum [84].

The two-component Bose-Hubbard model in the strong-coupling regime ($U \gg t$, $U > U_{AB}$) presents a MI as the ground state with total filling $\nu = \nu_A + \nu_B$ (we concentrate on the case $\nu_A = \nu_B = 1$). This is a gapped phase and we expect that the boundary-linked perturbation theory presented in [83] will be reliable. Within this theory the ES is characterized by a low-lying value (the dominant one) which represents the MI state. Excited states in the ES are given by excitations over the MI state which can be obtained through ordinary perturbation theory on the wavefunction considering the hopping Hamiltonian as a perturbation. First excited states in the ES are associated with excitations over the boundary separating the two subsystems A and B. Higher excited states in the ES are related with higher orders in perturbation theory associated with processes further away from the boundary (bulk processes). This reflects the boundary nature of the ES because low-lying states correspond with excitations close to the boundary.

Analytical expressions for the lowest eigenvalues of the ES are easily obtained, here we present the results up to second-order perturbation theory (we set an energy scale $t = 1$)

$$\begin{aligned} \xi_1 &= 2\log U - \log 2, \\ \xi_2 &= 2\log\left(U^2 \pm U U_{AB}\right) - \log 4. \end{aligned} \tag{53}$$

It is interesting to note that the first excited value is the same than the one given in the one-component Bose-Hubbard [83]. This is directly related (in this perturbation theory) with the fact that the energy of the first excitation does not depend on U_{AB}. Then, the associated ES value will remain constant if U does not vary. This first excited state has a degeneracy equal to 4, corresponding to the fact that an A boson can jump over the boundary to the left or to the right and the same for a B boson.

Since our Hamiltonian has a $U(1) \times U(1)$ symmetry (corresponding to the number conservation for each type of bosons) we can use the number of bosons A and B to characterize our ES, specifically since we are studying excitations over the MI we introduce the quantum numbers $\delta N_A = N_A - L/2$ and $\delta N_B = N_B - L/2$ which represent the excess ($\delta N_i > 0$) or absence ($\delta N_i < 0$) of bosons $i = A, B$ with respect to the MI with total filling $\nu_A = \nu_B = 1$, on the left subsystem. For example, the four-degenerated first excited states are characterized by $\delta N_A = \pm 1$; $\delta N_B = 0$ and $\delta N_A = 0$; $\delta N_B = \pm 1$. Coming back to the second lowest eigenvalues in (53) we show the corresponding boson

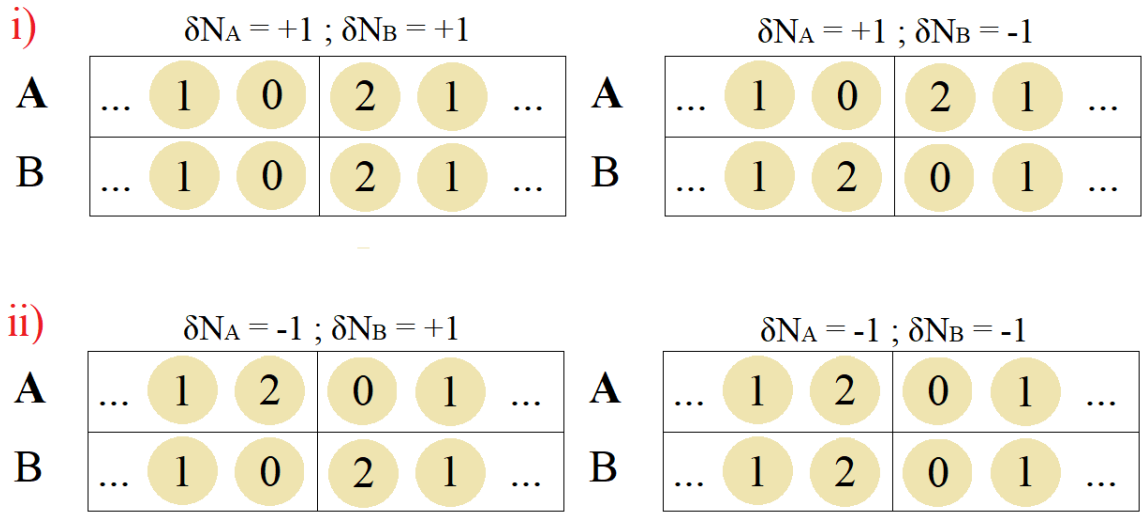

Figure 7. Configurations corresponding to the values labeled i and ii of the entanglement spectrum Fig. 8.

configurations in Fig. 7. One can see that these are of two types: the ones with $\delta N_A = \delta N_B$ which favor the movement of two different bosons over the boundary in the same direction or the ones with $\delta N_A = -\delta N_B$ which favor the hopping of two different bosons over the boundary in opposite directions. The first ones are associated with the $+$ solution and the second ones with the $-$ one in Eq.(53). Configurations with $\delta N_A = -\delta N_B$ are very special since they separate the two components along the boundary, and this is a reminiscent mechanism of the phase separation predicted at $U_{AB} = U$. In fact, from our analytical results Eq. (53) we predict that the ES value associated with these configurations becomes of the same order than the MI one $\xi_0 \approx 0$ for $U_{AB} = \frac{U^2-2}{U} \approx U$ in the strong coupling regime $U \gg t = 1$. This is associated with a closure of the Schmidt gap [85], namely the two largest Schmidt values become degenerated. Therefore, we have shown a direct connection between the ES and the phase separation of the two-component system.

In order to verify our analytical expressions (53) we present a DMRG study of the two-component Bose-Hubbard model. We performed direct numerical simulations using $m = 150$ states of the reduced density matrix, leading to discarded weights lower than 10^{-8} and we allowed for a maximum occupancy of 4 bosons of each type in every site. First of all, we present a numerically obtained ES in Fig. 8 for null intercomponent interaction, $U_{AB} = 0$, using the good quantum numbers δN_A and δN_B. We can see that the low-lying spectrum looks as predicted by the perturbation theory: an almost zero value $\xi \approx 0$ corresponding to the MI, 4 degenerated values given by ξ_1 in Eq. (53) and associated with first order perturbation theory in the hopping; and finally the second lower values are fully 4 degenerated at $U_{AB} = 0$ and they are associated with second order perturbation theory which is totally absent in the single-component case [83].

In Fig. 9 we present the ES but for a non-zero value of the intercomponent

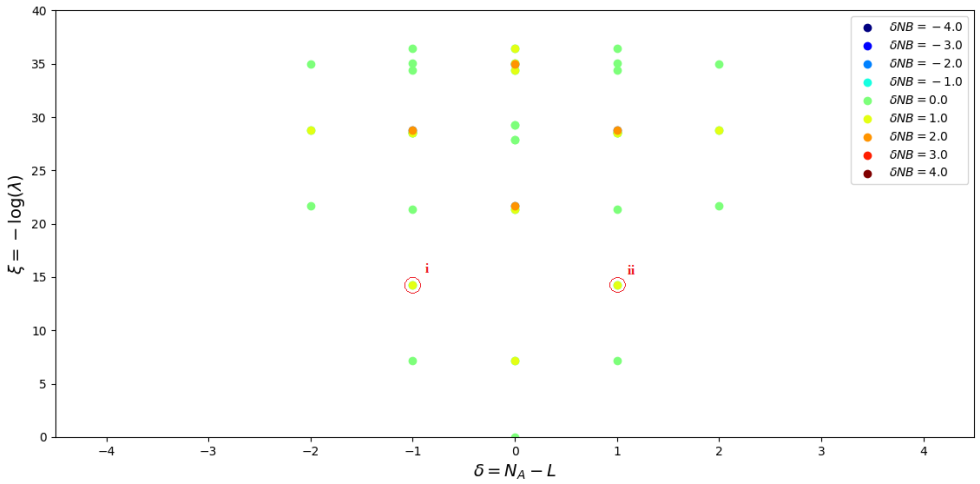

Figure 8. Entanglement spectrum for the Bose-Bose mixture with intracomponent interaction $U_A = U_B = 50$, hopping term $t_A = t_B = 1$ and intercomponent interaction $U_{AB} = 0$. δN_A and δN_B represents the excess ($\delta N > 0$) or absence ($\delta N < 0$) of δN particles in the left hand partition of the system. The first 'excited' levels correspond to the typical configurations for a single Bose-Hubbard model, where a particle of one species jumped across the boundary. The second levels i and ii correspond to configurations where a particle of each species jumped across the boundary (these configurations are not present in the single case). In Fig 7 we represent these configurations. They are degenerated since $U_{AB} = 0$ and particles from different species are not interacting.

interaction $U_{AB} = 5$. As predicted, the degeneracy in the first levels remains unchanged but in the second levels it is broken in pairs. Specifically, configurations with $\delta N_A = -\delta N_B = 1$ are favored against $\delta N_A = \delta N_B = 1$. We expect that this mechanism will be present in the higher part of the spectrum despite we are not presenting here explicit calculations in perturbation theory for higher values than the second one. But we can appreciate in Fig. 9 how multiple states break their degeneracy for non-zero values of U_{AB}, showing that some configurations are favored against other ones. Then, the interpretation for this two-component system is not as simple as for the one-component in the strong coupling limit. Despite the fact that we are in a regime where perturbation theory is reliable, the spacing between different levels corresponding to different orders in perturbation theory is not identical for all levels due to the interaction between the two components. This creates a richer structure in the ES, for example the second order in perturbation theory (decreases with U_{AB}) at some point will cross the first one (constant in U_{AB}).

This richer structure of the ES has to be explored at fixed U varying the intercomponent interaction U_{AB}. This is presented in Fig. 10 where we show this dependence of the ES comparing numerical results obtained through DMRG with our analytical results Eq. (53). First of all we observe that our analytical predictions are in

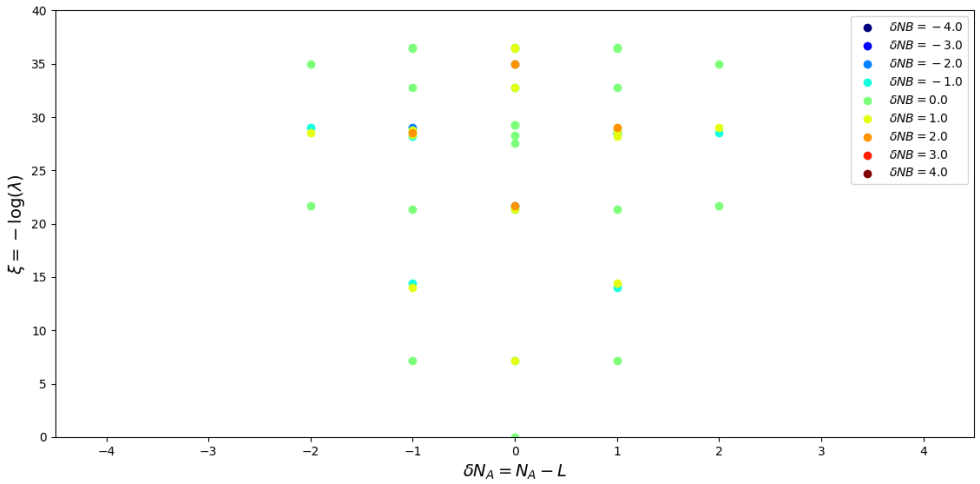

Figure 9. Entanglement spectrum for the Bose-Bose mixtures with intracomponent interaction $U_A = U_B = 50$, hopping term $t_A = t_B = 1$ and intercomponent interaction $U_{AB} = 5$. Intercomponent interactions break the degeneration in the second level. Now states with $\delta N_A = +1$, $\delta N_B = -1$ and $\delta N_A = -1$, $\delta N_B = +1$ are favored against $\delta N_A = +1$, $\delta N_B = +1$ and $\delta N_A = -1$, $\delta N_B = -1$.

total agreement with the numerical results in all the range $U_{AB} < U$ and $U \gg t$. In fact, we expect that the perturbation theory will be reliable as long as the intercomponent interaction is lower than the critical point predicted from this one $U_{AB} < \frac{U^2-2}{U} = 49.96$ for $U = 50$. We observe how multiple degenerated states at $U_{AB} = 0$ are split when one turns on the intercomponent interaction. If this interaction is increased, different orders in perturbation theory decrease, specifically there is a crossing between the second and first ones at $U_{AB} \approx 49$. As one approaches the critical point $U_{AB} = U$, arbitrary higher orders in perturbation theory become comparable to the MI state. This point which marks the transition to phase separation is an special one and it has to be studied independently.

Once studied the ES in the whole region $U \gg t$ and $0 \leq U_{AB} < U$ showing the non-trivial perturbative interpretation of the ES, now we move to the critical point $U_{AB} = U$. This is an special point because the symmetry of the interacting part of the Hamiltonian (without hopping) Eq. (52) $U(1) \times U(1)$ is enlarged to $U(1) \times SU(2)$. This is reflected in the fact that any state with fixed number of total particles N is fully degenerated in the thermodynamic limit with any combination $N_A + N_B = N$ being $N_A = N - N_B$. Then there is a submanifold where the ground state in the thermodynamic limit is infinitely degenerated, and it is constructed under the constrain of N constant. The important point is that the DMRG is constructed implementing the symmetry $U(1) \times U(1)$ and we fixed the number of particles for each species N_A and N_B. The ground state generated by our algorithm will explicitly break the symmetry of the Hamiltonian at the critical point (this is also expected in real experiments) selecting one particular direction of

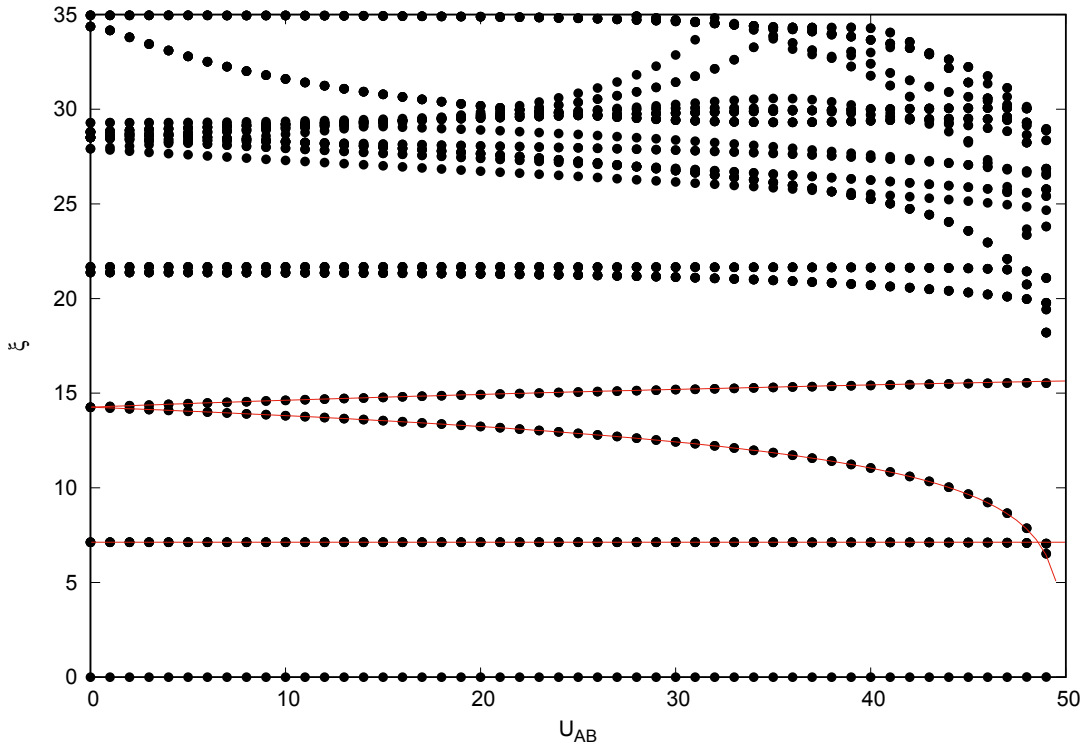

Figure 10. Entanglement spectrum $\xi = -\log\lambda$ at fixed total size $L = 64$ as a function of the intercomponent interaction U_{AB} for fixed value of the intracomponent one $U = 50$. Continuous red lines represent analytical results Eqs. (53) obtained through first and second order perturbation theory.

the fully degenerated subspace, specifically selecting the $N_A = N_B = N/2$ one. In finite systems the broken symmetry is partially restored and the low-energy spectrum acquires a particular form, often called an *Anderson tower* or a *Tower of states* (TOS). The full degeneracy is broken in a finite system and in the energy spectrum appears a TOS which becomes fully degenerated as one approaches the thermodynamic limit. This one is often separated from a continuous high-energy part by a gap which remains finite in the thermodynamic limit. The observation of this TOS structure has been used (TOS spectroscopy) to detect symmetry broken phases in finite systems [86, 87, 88, 89].

We present the ES for the two-component Bose-Hubbard Eq. (52) at the critical point $U = U_{AB}$ in Fig. 11 using linear combinations of the two quantum numbers δN_A and δN_B. We have observed that there is a sudden change in the structure of the ES as long as one approaches the critical point $U = U_{AB}$. We can observe that there is a correspondence between the energy TOS structure and this one. In terms of the total number of particles $\delta N_A + \delta N_B$ the entanglement spectrum reflects a MI behavior, in the sense that states at different number of total particles are separated by a gap. The fact that we have a two-component system is reflected in the existence of an internal structure in each sector with fixed δN, the TOS. This structure is given by any possible

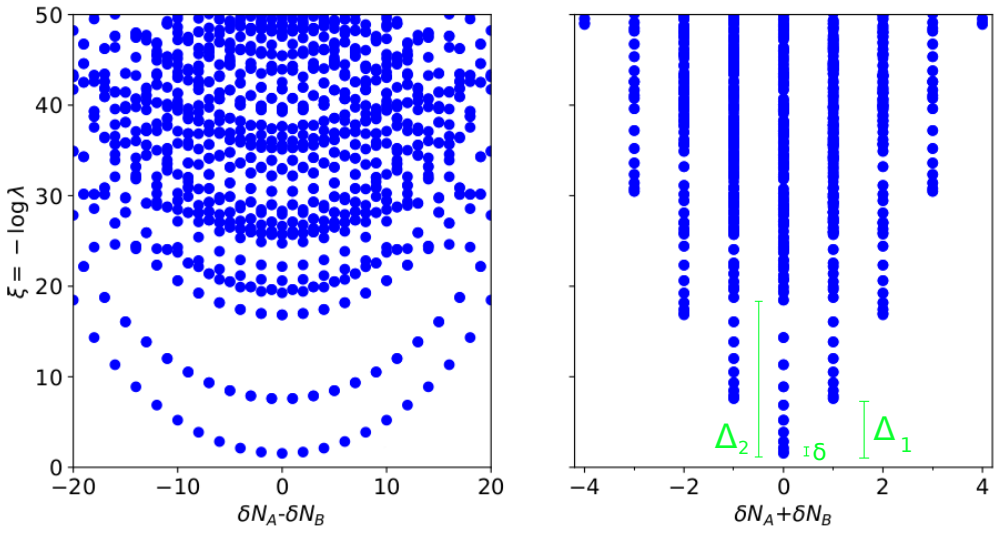

Figure 11. Entanglement spectrum of the two-component Bose-Hubbard model at the critical point $U = U_{AB} = 50$ at fixed system size $L = 64$. We use combinations of the two quantum numbers δN_A and δN_B, the sum on the left panel and the subtraction on the right one. On the right panel we represent (green color) the different gaps defined in text.

combination of δN_A and δN_B satisfying that the value of their sum is δN. These towers are separated from a continuum by a gap. For example, the structure satisfying that $\delta N_A + \delta N_B = 0$ presents a TOS which in the representation of $\delta N_A - \delta N_B$ gives the lowest branch which has a parabolic shape. The second ones are given by $\delta N_A + \delta N_B = \pm 1$ and in the representation $\delta N_A - \delta N_B$ they give the second parabola which is double degenerated.

This connection between the TOS structure of the energy spectrum and the ES one has been recently observed. Specifically, in 2D systems with the ground state spontaneously breaking a symmetry, the lower part of the ES is structured as a TOS one [90, 91]. In our system, despite we have a one-dimensional system where this theory does not seem applicable, the fact that we have two different internal states has been shown to play the role of an extra dimension[92]. The two internal degrees of freedom, A and B, can be re-interpreted as playing the role of two one-dimensional systems coupled forming a two-dimensional one, with, in this case, a very small second dimension.

Now we characterize the properties of the entanglement spectrum, see Fig. 11. In order to do that we define the *envelope gap* $\delta = \xi_0(\delta N_A - \delta N_B = \pm 2) - \xi_0(\delta N_A - \delta N_B = 0)$, the gap between two tower of states $\Delta_1 = \xi_0(\delta N_A - \delta N_B = \pm 1) - \xi_0(\delta N_A - \delta N_B = 0)$ and the gap with the continuum $\Delta_2 = \xi_1(\delta N_A - \delta N_B = 0) - \xi_0(\delta N_A - \delta N_B = 0)$, see Fig. 11. In Fig. 12 we represent the envelope gap δ and we can observe a linear dependence with $1/L$, which is expected for a two-dimensional system [90, 91]. In general, for a d-dimensional system: $\delta \sim L^{1-d}$. We observe that the gap is non-vanishing in the thermodynamic limit, this is not surprising since despite the fact that

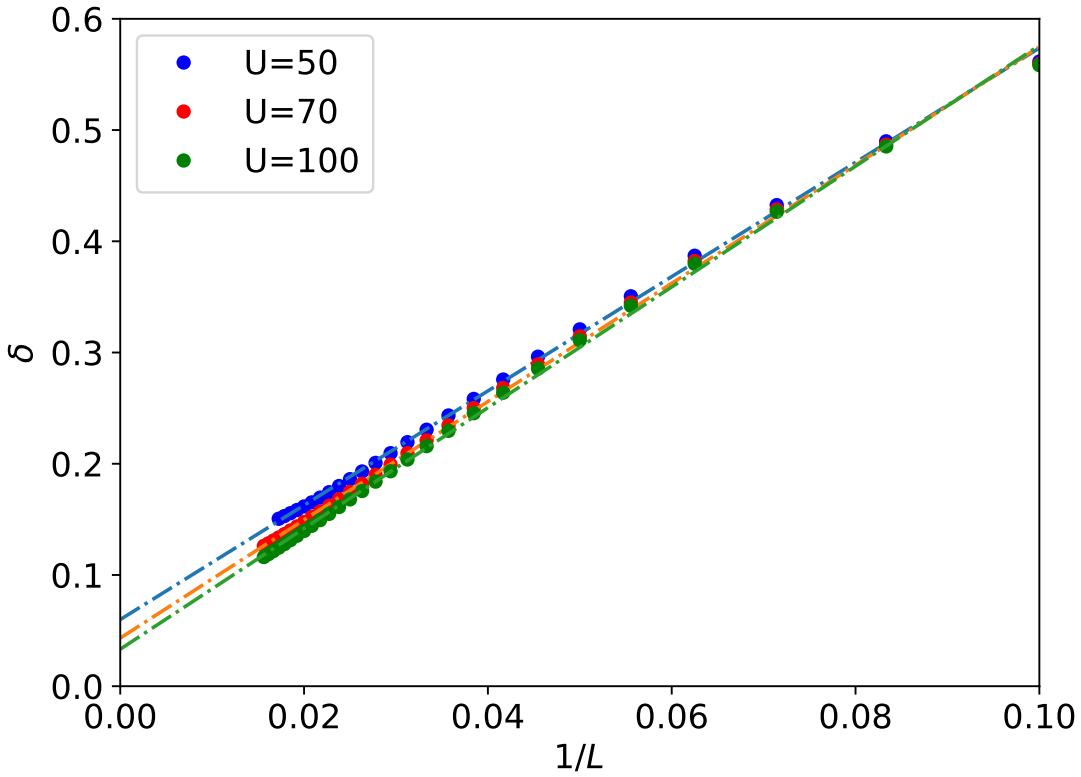

Figure 12. Envelope gap (defined in text) at the critical point $U = U_{AB}$ as a function of the inverse of the size chain L. The results are obtained through DMRG algorithm (dots). We represent different values of the intracomponent interaction at fixed $t = 1$. Linear fittings are represented by dashed-dotted lines.

we are in a strong-coupling regime the hopping part of the Hamiltonian is non-vanishing and partially breaks the $SU(2)$ symmetry between the components. Taking the limit $U/t \to \infty$ the $SU(2)$ symmetry of our Hamiltonian will be restored. In Fig. 13 we represent the envelope gap obtained in the thermodynamic limit $\delta(L \to \infty)$ assuming the linear dependence on $1/L$. The linear dependence on $1/U$ comes from the fact that in the strong-coupling regime a second hopping provides an energy proportional to this factor. As we have anticipated, the envelope gap becomes totally vanishing in the thermodynamic limit and for $U/t \to \infty$, where the SSB is fully produced. In this limit we expect a full degeneracy in each TOS structure.

We have observed that the gaps Δ_1 and Δ_2 do not present an explicit dependence on the system size, although we can not exclude a weaker dependence such as a logarithmic one, but they remain finite in the thermodynamic limit. On the other hand, there is a strong dependence of these gaps on the intracomponent interaction U, in Fig. 14 we observe a linear dependence. This reflects the MI nature of the system in terms of the quantum number $\delta N_A + \delta N_B$. Adding a particle into the system gives a non-vanishing energy proportional to the on-site intracomponent/intercomponent interaction

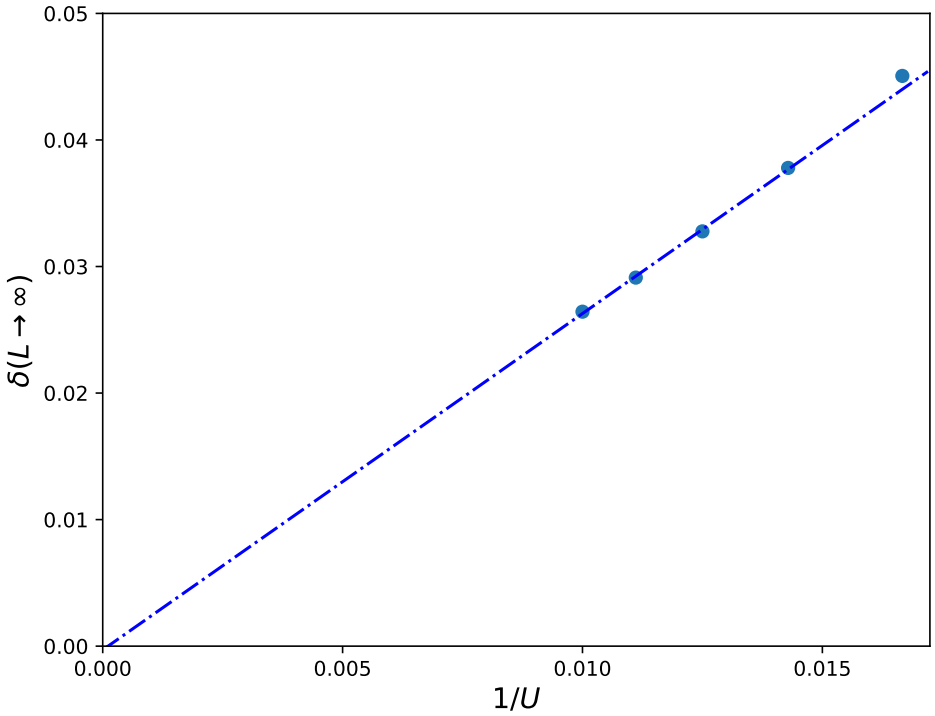

Figure 13. Envelope gap in the thermodynamic limit $\delta(L \to \infty)$ (dots) obtained through linear extrapolations of Fig. 12. The dependence on the intracomponent interaction U is linear in $1/U$. Dashed-dotted line represents a linear fitting.

$U = U_{AB}$.

The direct connection presented above between the ES and the true energy

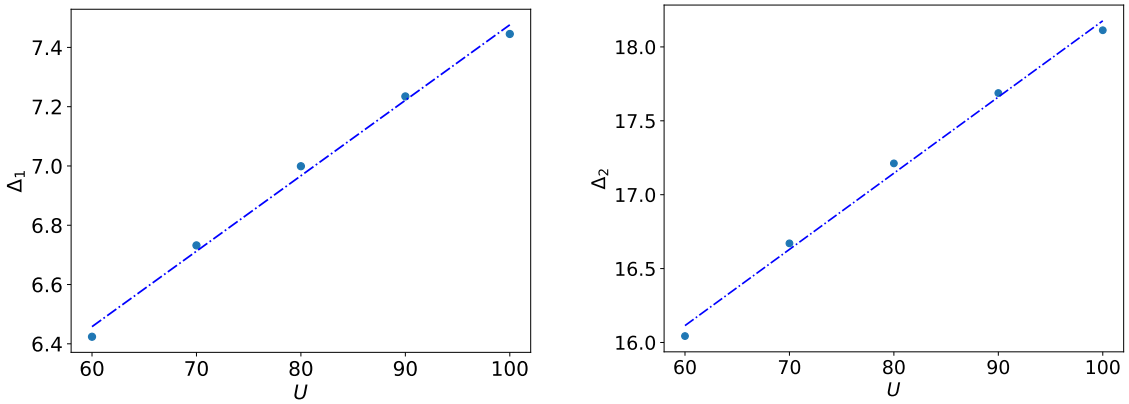

Figure 14. Gaps Δ_1 and Δ_2 (defined in text) at the critical point $U = U_{AB}$ as a function of the intracomponent interaction U at fixed total size $L = 64$. Dashed-dotted line represents a linear fitting.

spectrum of the Hamiltonian can be used as a mechanism to detect phase transitions. This is very useful in the sense that, we only need the groundstate of the system to fully characterize the phase at which the system is present. Specifically, here we have shown how the entanglement spectrum drastically changes at the critical point $U = U_{AB}$ which is exactly the point at which the phase separation transition is produced.

5. Conclusions and Outlook

In this work we have presented a study of the Bose-Hubbard model. First, we have reviewed the single-component case introducing theoretical techniques to characterize the two different phases: the Mott insulator and the superfluid phase; and the quantum phase transition (QPT) between them. We have also implemented a Density Matrix Renormalization Group (DMRG) algorithm to numerically simulate this model and we have introduced entanglement properties to characterize the QPT.

We have also studied the two-component Bose-Hubbard model via a DMRG algorithm. More specifically, we have studied the entanglement properties in the strong-coupling regime. The lower part of the entanglement spectrum has been analytically obtained performing a linked-perturbation theory in the whole range except at the critical point where the strength of the intracomponent interactions equals the intercomponent one. These analytical results have been compared with DMRG simulations, showing a very good agreement. We have observed a non-trivial dependence on the entanglement spectrum as a function of the intercomponent interaction, predicting a closure of the entanglement gap as one approaches the critical point where phase separation is expected. In fact, the structure of the entanglement spectrum drastically changes at this point, revealing an Anderson tower of states. This one has been extensively studied as a function of the intracomponent interactions and the system size.

To the best of our knowledge this is the first time that an Anderson tower of states is reported in the entanglement spectrum of a multicomponent one-dimensional system. We have argued how these systems can mimic higher dimensional ones and how this is reflected in the entanglement spectrum. In particular, the direct connection between the entanglement spectrum and the energy spectrum in multicomponent systems could allow for detecting phases which are explicitly connected with this multicomponent nature, like we have done with the phase separation one. It would be interesting to extend our results to the weakly-interacting regime. We know that the phase diagram of the two-component Bose-Hubbard is very rich, presenting new phases like the superfluid-counterflow. Entanglement properties of these regions are still unknown.

References

[1] Anderson M H, Ensher J R, Matthews M R, Wieman C E and Cornell E A 1995 *Science* **269** 198–201

[2] Bradley C C, Sackett C A, Tollett J J and Hulet R G 1995 *Phys. Rev. Lett.* **75**(9) 1687–1690

[3] Davis K B, Mewes M O, Andrews M R, van Druten N J, Durfee D S, Kurn D M and Ketterle W 1995 *Phys. Rev. Lett.* **75**(22) 3969–3973

[4] Pitaevskii L P 2003 *Bose-Einstein condensation* (Oxford New York: Clarendon Press)

[5] Pethick C 2008 *Bose-Einstein condensation in dilute gases* (Cambridge New York: Cambridge University Press)

[6] Jaksch D, Bruder C, Cirac J I, Gardiner C W and Zoller P 1998 *Phys. Rev. Lett.* **81**(15) 3108–3111

[7] Altland A 2010 *Condensed Matter Field Theory* (Leiden: Cambridge University Press)

[8] Essler F 2005 *The one-dimensional Hubbard model* (Cambridge: Cambridge University Press)

[9] Fisher M P A, Weichman P B, Grinstein G and Fisher D S 1989 *Phys. Rev. B* **40**(1) 546–570

[10] Bloch I, Dalibard J and Zwerger W 2008 *Rev. Mod. Phys.* **80**(3) 885–964

[11] Moritz H, Stöferle T, Köhl M and Esslinger T 2003 *Phys. Rev. Lett.* **91**(25) 250402

[12] Greiner M, Bloch I, Mandel O, Hänsch T W and Esslinger T 2001 *Phys. Rev. Lett.* **87**(16) 160405

[13] Kinoshita T, Wenger T and Weiss D S 2004 *Science* **305** 1125–1128

[14] Inouye S, Andrews M R, Stenger J, Miesner H J, Stamper-Kurn D M and Ketterle W 1998 *Nature* **392** 151 EP – article

[15] Courteille P, Freeland R S, Heinzen D J, van Abeelen F A and Verhaar B J 1998 *Phys. Rev. Lett.* **81**(1) 69–72

[16] Chin C, Grimm R, Julienne P and Tiesinga E 2010 *Rev. Mod. Phys.* **82**(2) 1225–1286

[17] Lewenstein M, Sanpera A and Ahufinger V 2012 *Ultracold Atoms in Optical Lattices: Simulating Quantum Many-body Systems* (Oxford, U.K: Oxford University Press)

[18] Sachdev S 2011 *Quantum phase transitions* (Cambridge New York: Cambridge University Press)

[19] Greiner M, Mandel O, Esslinger T, Hänsch T W and Bloch I 2002 *Nature* **415** 39 EP – article

[20] Osborne T J and Nielsen M A 2002 *Phys. Rev. A* **66**(3) 032110

[21] Osterloh A, Amico L, Falci G and Fazio R 2002 *Nature* **416** 608 EP –

[22] Vidal G, Latorre J I, Rico E and Kitaev A 2003 *Phys. Rev. Lett.* **90**(22) 227902

[23] Ladd T D, Jelezko F, Laflamme R, Nakamura Y, Monroe C and O'Brien J L 2010 *Nature* **464** 45 EP – review Article

[24] Bloch I 2005 *Nature Physics* **1** 23 EP – review Article

[25] Ashcroft N 1976 *Solid state physics* (New York: Holt, Rinehart and Winston)

[26] Stoof H 2009 *Ultracold quantum fields* (Dordrecht Bristol: Springer in association with Canopus Pub)

[27] Gribakin G F and Flambaum V V 1993 *Phys. Rev. A* **48**(1) 546–553

[28] Flambaum V V, Gribakin G F and Harabati C 1999 *Phys. Rev. A* **59**(3) 1998–2005

[29] Bogolyubov N N 1947 *J. Phys.(USSR)* **11** 23–32 [Izv. Akad. Nauk Ser. Fiz.11,77(1947)]

[30] Gross E P 1961 *Il Nuovo Cimento (1955-1965)* **20** 454–477 ISSN 1827-6121

[31] Pitaevsk L P 1961 *Soviet Physics JETP-USSR* **13**

[32] Marzari N, Mostofi A A, Yates J R, Souza I and Vanderbilt D 2012 *Rev. Mod. Phys.* **84**(4) 1419–1475

[33] Gross C and Bloch I 2017 *Science* **357** 995–1001

[34] Rey A M, Burnett K, Roth R, Edwards M, Williams C J and Clark C W *Journal of Physics B: Atomic, Molecular and Optical Physics* **36** 825

[35] van Oosten D, van der Straten P and Stoof H T C 2001 *Phys. Rev. A* **63**(5) 053601

[36] Mermin N D and Wagner H 1966 *Phys. Rev. Lett.* **17**(22) 1133–1136

[37] Hohenberg P C 1967 *Phys. Rev.* **158**(2) 383–386

[38] Mermin N D 1968 *Phys. Rev.* **176**(1) 250–254

[39] Dettmer S, Hellweg D, Ryytty P, Arlt J J, Ertmer W, Sengstock K, Petrov D S, Shlyapnikov G V,

Kreutzmann H, Santos L and Lewenstein M 2001 *Phys. Rev. Lett.* **87**(16) 160406
[40] Ginzburg V L and Landau L D 1950 *Zh. Eksp. Teor. Fiz.* **20** 1064–1082
[41] Wilson K G 1975 *Rev. Mod. Phys.* **47**(4) 773–840
[42] White S R 1992 *Phys. Rev. Lett.* **69**(19) 2863–2866
[43] Schollwöck U 2005 *Rev. Mod. Phys.* **77**(1) 259–315
[44] De Chiara G, Rizzi M, Rossini D and Montangero S 2006 *eprint arXiv:cond-mat/0603842* (*Preprint* `cond-mat/0603842`)
[45] Schollwöck U 2011 *Annals of Physics* **326** 96 – 192 ISSN 0003-4916 january 2011 Special Issue
[46] Vidal G 2003 *Phys. Rev. Lett.* **91**(14) 147902
[47] Orús R and Latorre J I 2004 *Phys. Rev. A* **69**(5) 052308
[48] Vidal G 2004 *Phys. Rev. Lett.* **93**(4) 040502
[49] Vidal G 2008 *Phys. Rev. Lett.* **101**(11) 110501
[50] Orús R and Vidal G 2009 *Phys. Rev. B* **80**(9) 094403
[51] Kashurnikov V A, Krasavin A V and Svistunov B V 1996 *Journal of Experimental and Theoretical Physics Letters* **64** 99–104 ISSN 1090-6487
[52] Kashurnikov V A and Svistunov B V 1996 *Phys. Rev. B* **53**(17) 11776–11778
[53] Pai R V, Pandit R, Krishnamurthy H R and Ramasesha S 1996 *Phys. Rev. Lett.* **76**(16) 2937–2940
[54] Kühner T D, White S R and Monien H 2000 *Phys. Rev. B* **61**(18) 12474–12489
[55] Roux G, Barthel T, McCulloch I P, Kollath C, Schollwöck U and Giamarchi T 2008 *Phys. Rev. A* **78**(2) 023628
[56] Cazalilla M A, Citro R, Giamarchi T, Orignac E and Rigol M 2011 *Rev. Mod. Phys.* **83**(4) 1405–1466
[57] Francesco P 1997 *Conformal field theory* (New York: Springer)
[58] Calabrese P and Cardy J 2004 *Journal of Statistical Mechanics: Theory and Experiment* **2004** P06002
[59] Holzhey C, Larsen F and Wilczek F 1994 *Nuclear Physics B* **424** 443 – 467 ISSN 0550-3213
[60] Affleck I and Ludwig A W W 1991 *Phys. Rev. Lett.* **67**(2) 161–164
[61] Laflorencie N, Sørensen E S, Chang M S and Affleck I 2006 *Phys. Rev. Lett.* **96**(10) 100603
[62] Fagotti M and Calabrese P 2011 *Journal of Statistical Mechanics: Theory and Experiment* **2011** P01017
[63] Cazalilla M A 2004 *Journal of Physics B: Atomic, Molecular and Optical Physics* **37** S1
[64] Läuchli A M and Kollath C 2008 *Journal of Statistical Mechanics: Theory and Experiment* **2008** P05018
[65] Gadway B, Pertot D, Reimann R and Schneble D 2010 *Phys. Rev. Lett.* **105**(4) 045303
[66] Catani J, De Sarlo L, Barontini G, Minardi F and Inguscio M 2008 *Phys. Rev. A* **77**(1) 011603
[67] Mandel O, Greiner M, Widera A, Rom T, Hänsch T W and Bloch I 2003 *Phys. Rev. Lett.* **91**(1) 010407
[68] Myatt C J, Burt E A, Ghrist R W, Cornell E A and Wieman C E 1997 *Phys. Rev. Lett.* **78**(4) 586–589
[69] Kuklov A B and Svistunov B V 2003 *Phys. Rev. Lett.* **90**(10) 100401
[70] Mathey L 2007 *Phys. Rev. B* **75**(14) 144510
[71] Hu A, Mathey L, Danshita I, Tiesinga E, Williams C J and Clark C W 2009 *Phys. Rev. A* **80**(2) 023619
[72] Mishra T, Pai R V and Das B P 2007 *Phys. Rev. A* **76**(1) 013604
[73] Lingua F, Guglielmino M, Penna V and Capogrosso Sansone B 2015 *Phys. Rev. A* **92**(5) 053610
[74] Zhan F, Sabbatini J, Davis M J and McCulloch I P 2014 *Phys. Rev. A* **90**(2) 023630
[75] Barbiero L, Abad M and Recati A 2016 *Phys. Rev. A* **93**(3) 033645
[76] Nicklas E, Strobel H, Zibold T, Gross C, Malomed B A, Kevrekidis P G and Oberthaler M K 2011 *Phys. Rev. Lett.* **107**(19) 193001
[77] Wang W, Penna V and Capogrosso-Sansone B 2016 *New Journal of Physics* **18** 063002
[78] Sarkar S, McEndoo S, Schneble D and Daley A J 2018 *ArXiv e-prints* (*Preprint* `1805.01592`)

[79] Li H and Haldane F D M 2008 *Phys. Rev. Lett.* **101**(1) 010504
[80] Nienhuis B, Campostrini M and Calabrese P 2009 *Journal of Statistical Mechanics: Theory and Experiment* **2009** P02063
[81] Läuchli A M, Bergholtz E J, Suorsa J and Haque M 2010 *Phys. Rev. Lett.* **104**(15) 156404
[82] Frérot I and Roscilde T 2016 *Phys. Rev. Lett.* **116**(19) 190401
[83] Alba V, Haque M and Läuchli A M 2012 *Phys. Rev. Lett.* **108**(22) 227201
[84] Läuchli A M 2013 *ArXiv e-prints* (*Preprint* 1303.0741)
[85] De Chiara G, Lepori L, Lewenstein M and Sanpera A 2012 *Phys. Rev. Lett.* **109**(23) 237208
[86] Bernu B, Lhuillier C and Pierre L 1992 *Phys. Rev. Lett.* **69**(17) 2590–2593
[87] Bernu B, Lecheminant P, Lhuillier C and Pierre L 1994 *Phys. Rev. B* **50**(14) 10048–10062
[88] Lecheminant P, Bernu B, Lhuillier C, Pierre L and Sindzingre P 1997 *Phys. Rev. B* **56**(5) 2521–2529
[89] Shannon N, Momoi T and Sindzingre P 2006 *Phys. Rev. Lett.* **96**(2) 027213
[90] Alba V, Haque M and Läuchli A M 2013 *Phys. Rev. Lett.* **110**(26) 260403
[91] Kolley F, Depenbrock S, McCulloch I P, Schollwöck U and Alba V 2013 *Phys. Rev. B* **88**(14) 144426
[92] Boada O, Celi A, Latorre J I and Lewenstein M 2012 *Phys. Rev. Lett.* **108**(13) 133001